THE EFFECT OF PRISMATIC ROUGHNESS ELEMENTS ON HYDRAULIC JUMP

A THESIS SUBMITTED TO
THE GRADUATE SCHOOL OF NATURAL AND APPLIED SCIENCES
OF
MIDDLE EAST TECHNICAL UNIVERSITY

BY

TAYLAN ULAŞ EVCİMEN

IN PARTIAL FULFILLMENT OF THE REQUIREMENTS
FOR
THE DEGREE OF MASTER OF SCIENCE

IN

CIVIL ENGINEERING

JANUARY 2005

Approval of the Graduate School of Natural and Applied Sciences

_____
Prof. Dr. Canan Özgen
Director

I certify that this thesis satisfies all the requirements as a thesis for the degree of Master of Science.

_____
Prof. Dr. Erdal ÇOKCA
Head of the Department

This is to certify that we have read this thesis and that in our opinion it is fully adequate, in scope and quality, as a thesis for the degree of Master of Science.

_____
Assoc. Prof. Dr. Nuray TOKYAY
Supervisor

Examining Committee Members

Prof. Dr. Ayşen ERGİN (METU, CE)_____

Assoc. Prof Dr. Nuray TOKYAY (METU, CE)_____

Prof. Dr. Tülay ÖZBEK (GAZİ UNI. CE)_____

Asst. Prof. Dr. Zafer BOZKUŞ (METU, CE)_____

Asst. Prof. Dr. Burcu Altan SAKARYA (METU, CE)_____

I hereby declare that all information in this document has been obtained and presented in accordance with academic rules and ethical conduct. I also declare that, as required by these rules and conduct, I have fully cited and referenced all material and results that are not original to this work.

Name, Last name : Taylan Ulaş Evcimen

Signature :

ABSTRACT

THE EFFECT OF PRISMATIC ROUGHNESS ELEMENTS ON HYDRAULIC JUMP

EVCİMEN, Taylan Ulaş

M. Sc., Department of Civil Engineering

Supervisor : Assoc. Prof. Dr. Nuray TOKYAY

January 2005, 82 Pages

The objective of this study is to determine the effect of different roughness types and arrangements on hydraulic jump characteristics in a rectangular channel. Three different types of roughness were used along experiments. All of them had rectangular prism shapes and that were placed normal to the flow direction. To avoid cavitation, height of roughness elements were arranged according to level of the channel inlet, so that the crests of roughness elements would not be protruding into the flow. The effects of roughness type and arrangement on hydraulic jump properties, i.e. energy dissipation, length of the jump and tail water depth were investigated. These properties were compared with the available data in literature and with the properties of hydraulic jump occurred on smooth bed.

Keywords : Hydraulic Jump, Energy Dissipation, Rough Beds, Prismatic Roughness

ÖZ

PRİZMATİK PÜRÜZLÜLÜĞÜN HİDROLİK SIÇRAMA ÜZERİNE ETKİLERİ

EVCİMEN, Taylan Ulaş
Yüksek Lisans, İnşaat Mühendisliği Bölümü
Tez Danışmanı : Doç. Dr. Nuray TOKYAY

Ocak 2005, 82 Sayfa

Bu çalışmada farklı pürüzlülük tiplerinin ve düzenlemelerinin dikdörtgen kanallardaki hidrolik sıçramalara olan etkisinin belirlenmesi amaçlanmıştır. Üç farklı tip pürüzlülük kullanılmıştır. Kullanılan bütün pürüzlülük tipleri dikdörtgenler prizması şeklindedir ve deneylerde akıma dik yerleştirilmişlerdir. Kavitasyondan korunmak için pürüzlülük yükseklikleri menba tabanının seviyesine göre düzenlenmiş, böylece pürüzlülük elemanlarının tepe noktalarının akımın içine girmemesi sağlanmıştır. Pürüzlülük tiplerinin ve düzenlemelerinin enerji sönümlenmesi, sıçrama uzunluğu ve sıçrama sonrası oluşan akım derinliği üzerindeki etkisi araştırılmıştır. Sonuçlar, literatürdeki bulunan verilerle ve pürüzsüz tabanda oluşan hidrolik sıçramanın özelikleriyle karşılaştırılmıştır

Anahtar Kelimeler : Hidrolik Sıçrama, Enerji Sönümlenmesi, Pürüzlü Taban, Prizmatik Pürüzlülük

To My Mother

"Düşünde bile göremez işler
Düşlerin gördüğü işleri"

ACKNOWLEDGEMENTS

This study has been carried out under the supervision of Assoc. Prof. Dr. Nuray TOKYAY in the Hydraulics Laboratory of the Department of Civil Engineering at the Middle East Technical University.

I wish to express my sincere gratitude to Assoc. Prof. Dr Nuray TOKYAY, the author's thesis advisor, for her guidance, supervision and encouragement in the course of preparation of the dissertation.

I would like to thank to Prof. Dr. Metin GER for his valuable comments and suggestions.

I would like to thank my Father M. Bülent EVCİMEN and my sister N. İlkem EVCİMEN for their patiance and unshakable faith in me.

My special thanks go to Gülfer KESKİN and Erdem TÜRKŞEN, who have motivated me psychologically in my works, supported me in all conditions and all times and thought how a good person should be.

Special thanks go to Barış YELDİREN, Şerif LEVENT, Serkan AYDINOĞLU, Cenk VAROL, Barış TÜRKMEN, Ümit İŞLER, Güneş GOLER, Murat SÜMER, Taner FIRTINA, Selçuk Han DÜLGEROĞLU, İlker GÜNDEZ, Köksal ŞAHİN and A. Jeni GÜNEŞ for their moral support.

I wish to express special thanks to Ayşe KARINCA, who always shares the joy and difficulties of life.

TABLE OF CONTENTS

LIST OF FIGURES

FIGURE **PAGE**

LIST OF TABLES

TABLE **PAGE**

LIST OF SYMBOLS

$\overline{S}$	Non dimensional bottom shear force,
a	Gate opening,
Cc	Contraction coefficient of V-notch,
D	$= (y_2^* - y_2) / y_2^*$, depth reduction factor,
E_1	Specific energy of supercritical flow,
E_2	Specific energy of subcritical flow,
E_L	Specific energy loss along hydraulic jump,
E_L^*	Specific energy loss along hydraulic jump on smooth beds,
F_1	Froude number of supercritical flow,
F_2	Froude number of subcritical flow,
g	Gravitational acceleration,
G	$= (E_L - E_L^*) / E_L$, Gain in energy dissipation factor,
H	Head measured on V-notch,
L	Length of roughness element,
L_J	Length of hydraulic jump,
L_J^*	Length of hydraulic jump,
L_R	Length of roller,
J	Downstream turbulance-flux correction factor,
q	Discharge per unit width of the flow,
Q	Volumetric discharge,
R_1^*	Modified Reynolds Number,
s	Wavelength of the corrugation,
S_f	Integrated dimensionless bed shear force per unit width,

T	$= (L_J^* - L_J) / L_J^*$ Gain in Length of Jump,
t	Height of corrugation,
V_1	Average flow velocity of supercritical flow,
w	Distance between two roughness element,
x	Space Parameter,
X_J	Starting point of hydraulic jump,
X	Horizontal length scale,
w	Length between two roughness element,
y	Space Parameter,
y_{CONT}	Flow depth at vena contracta,
y_R	Turning point of flow in hydraulic jump,
y_1	Depth of supercritical flow,
y_2	Depth of subcritical flow on rough beds,
y_2^*	Depth of supercritical flow on smooth beds,
Y	Sequent depth ratio,
z	Height of a roughness element,
α	Notch angle,
β_1	Momentum correction coefficient at the beginning of jump,
β_2	Momentum correction coefficient at the end of jump,
δ	Boundary layer height,
ρ	Mass density of water,
υ	Kinematic viscosity of water,

CHAPTER I

INTRODUCTION

1.1 Introduction

A hydraulic jump is the abrupt change of flow depth in the direction of flow in an open channel flow under certain conditions, where flowing stream passes from supercritical flow to subcritical flow *(Chow, 1959)*. Although Leonardo da Vinci (1452-1519) was the first person who mentioned the hydraulic jump, it was investigated for the first time at 1818 experimentally by Bidone.

In hydraulic structures, such as spillways and sluice gates, flow velocities are high at the downstream. Excess energy of flowing water should be dissipated to prevent downstream of these structures from scouring. These structures are the most common features, where the hydraulic jump is used as an energy dissipator. Furthermore, the hydraulic jump may be used for different purposes, such as operation of flow-measurement flumes to increase efficiency, mixing of chemicals to streams, desalination of sea water and aeration of streams which are polluted by bio-degradable wastes.

In design of stilling basins, on which hydraulic jump takes place, the length and the elevation of the basin are the most important parameters. These parameters are determined by the properties of the hydraulic jump. The bottom of the basin is paved to resist scouring; and stilling basin is rarely designed to

confine the entire length of the jump, because such a basin would be too expensive *(Chow, 1959).* The most effective design of stilling basin depends on shortness of the length of jump, the lowness of the elevation of jump and the stability of jump to make the apron height and length as small as possible. In order to satisfy those requirements, usually devices such as sills, baffle blocks etc. are installed into basin. Those devices are useful to fix the location of jump and reduce the length of jump.

The location of the hydraulic jump is determined by the force equilibrium between the supercritical upstream flow and the subcritical downstream flow. Conditions of tailwater depth and jump type are determined by the upstream supercrital flow's Froude number, which is the most important criteria for selection of type of stilling basin. When the Froude number of supercritical stream is greater than 10, hydraulic jump is no longer the most economical way of dissipation of energy because of high tailwater requirement.

Use of roughness elements on stilling basins increases the internal friction of jump and may become an important parameter in force equilibrium. However, because of the high velocity of incoming flow, if the roughness elements protrude into flow, cavitation causes erosion on roughness elements; the internal friction of jump decreases, consequently the jump may move downstream of basin. If downstream of basin bed is not paved, this causes erosion and possible damage to structure itself *(Ead and Rajaratnam, 2002)*.

Roughness elements, placed on stilling basins, increase the internal friction of the jump despite the fact that the crests of the roughness elements have the same level with upstream bed. Moreover, use of roughness elements buried in channel bed protects the roughness elements from cavitation when compared with cavitation on roughness elements in the case of protruding roughness.

1.2 Literature Review

Perry at al.(1969) studied the turbulent boundary layer over a wall roughened by transverse ribs, and proposed to divide the roughness into two types; k-type and d-type. In k-type roughness, roughness function determined by the height of the roughness, k, whereas in d-type roughness, height of roughness element is not important. The main agents on roughness function are boundary layer thickness, pipe diameter or channel height.

Hughes and Flack (1984) investigated hydraulic jump characteristics over several artificial roughened beds in a horizontal rectangular channel. They used seven different rough beds; the first of those was a series of parallel square bars aligned perpendicularly to the direction of flow, the second one was closely packed gravel particles cemented to the Plexiglas base and other five artificially roughened test beds were fabricated, by cementing roughness elements to a Plexiglas base. They used hypothetical plane, or effective bottom for gravel or artificial roughened beds, however they assumed that effective channel bottom coincides with the tops of the strip elements. Their experiments showed that the reduction in tail water depth and the length of jump is related to both the initial Froude number and the degree of roughness.

Tani(1987) suggested that, for regularly spaced ribs, difference between k-type and d-type roughness might be made at the pitch ratio w/z=4, where w is the pitch between the roughness elements and z is the height of the roughness. For d-type roughness, typified by closely spaced ribs with w/z less than 4.

Hager and Bremen (1989) analyzed the effect of wall friction on the sequent depths ratio both theoretically and experimentally. They stated that sequent depths of hydraulic jumps in laboratory studies have always slight disagreement with Belanger equation. They expressed that, flows with small incoming depths indicate the existence of a significant scale effect and in

model studies and there must be a limit for this scale. They proposed that a 5% deviation from the Belanger equation in model studies seems to reflect the accuracy on which a design might be based on. However they also stated that, for deviations greater than 5%, viscosity effects must be taken into account. They suggested an equation for the determination of jump whether it is influenced by scale effect or not.

Mohamed Ali (1991) has investigated hydraulic jump length on a rough channel bed. He has attempted to determine the optimum length of jump hydraulically and economically. In the experiments cubic roughness elements were used and the statistical methods have been used to obtain practical equations. He has found that the most efficient length of roughness is L/z = 28, where L is the length of roughness, and z is the height of roughness elements while relative roughness area is 10% of the bed surface. It was found that the length of jump was not related to roughness height ratio.

Ead et al (2000) investigated velocity field in turbulent open channel flow in circular corrugated culverts. They indicated that corrugations increase Reynolds shear stress and cause intense mixing along in the plane of the crests. They also pointed out velocity near the boundaries are smaller than average velocity of the flow significantly.

Ead and Rajaratnam (2002) investigated the effect of corrugations on length of the jump L_J, tailwater depth y_2, integrated bed shear stress $F\tau$, and dimensionless depth deficit parameter D in rectangular channels. They examined the effect of corrugations with Froude numbers from 4 to 10 and for three relative roughness t/y_1 values, where t is the amplitude of the corrugations and y_1 is the initial depth of the jump. They stated that the tail water depth required to form a jump on corrugated beds is appreciably smaller than that for the smooth beds, the length of jump on corrugations is about half of classical jump and integrated bed shear stress is about ten times that on

corrugated beds. Furthermore they also stated that the corrugations acted like cavities and the t/y_1 values have no effect on sequent depth ratio y_2/ y_1.

Negm (2002) has investigated the effect of roughness on the length of a hydraulic jump. A design equation was developed for the optimal length of stilling basin with cubic roughness elements. The equation contains flow and roughness parameters such as the initial Froude number, the height of roughness ratio, the length of roughness ratio, the initial length ratio, and the roughness density. Different intensities and heights of roughness and different roughened bed lengths were considered. The design equations that could be used to predict tailwater depth and length of jump on a bed with prismatic roughness were given.

Cui at al. (2003) investigated turbulent flow over rough surfaces for different pitch values between roughness elements. They used ribs as roughness elements and examined turbulence structure, the interaction between the roughness layer and outer flow, flow in the roughness layer and the roughness function associated with the time- and space- averaged velocity profile. They denoted that, for d-type roughness streamlines beyond the rib height and cavity nearly parallel; for intermediate roughness, w/z= 4, streamlines above the cavity are nearly parallel except near the rib and for k-type roughness, flow separates at four points between the roughness element.

Çelik et al. (2003) have investigated the effect of prismatic roughness elements on hydraulic jump properties. They stated that both the length and the sequent depth of a hydraulic jump in a rough channel are smaller than the length and sequent depth of a jump on a smooth channel.

Ayanlar (2004) investigated effect of corrugated beds on the properties of hydraulic Jump. He used corrugated aluminum sheets with different

wavelengths and F_1, incoming Froude number in the experiments with a range of $4 \leq F_1 \leq 12$. He found that corrugations reduce the required tail water depth for given upstream conditions, y_1 and F_1, when compared with the results of the hydraulic jumps on smooth bed. He stated that an average reduction factor for tail water depth is about 20% and the decrease in the length of hydraulic jump is about 35%. He also stated that G, the gain in energy loss for jumps on corrugated beds decreases as Froude number increases and tends to be constant at a value 7 % when the Froude number is greater than 8.

1.3 Scope of the Study

The aim of the present study is to investigate the effect of rectangular blocks on hydraulic jump properties i.e. sequent depth ratio, length of the jump, height of the jump and energy dissipation along jump when crests of the roughness elements have the same level with the supercritical stream at upstream bed. Furthermore effect of roughness height and spacing between roughness elements on hydraulic jump properties are studied by using different roughness height in the experiments.

Basic information on hydraulic jump is given in Chapter II. Experimental setup and experiments conducted are given in Chapter III. The results and discussion of results are given in Chapter IV. In Chapter V, discussions and conclusions are presented.

In Appendix A, experimental data taken in the present study is presented. In Appendix B, experimental data of Ead and Rajaratnam (2002), Ayanlar (2004) and length of jump data given by U.S.B.R. (1955) are presented. Experimental data of calibration of the triangular weir is given in Appendix C.

CHAPTER II

BASIC INFORMATION ON HYDRAULIC JUMP

2.1 Basic Characteristics of Hydraulic Jump

The basic characteristic of a hydraulic jump, such as i) the conjugate depths, ii) the energy loss in the jump, iii) the length of the jump, iv) the water surface profile of the jump, v) the velocity distribution of the jump will be given briefly in the following sections.

2.1.1 Conjugate Depths

For a simple hydraulic jump on a smooth rectangular channel shown in Fig. 2.1, the momentum equation along the flow direction will give the well-known Belanger equation *(Chow, 1959)*:

$$\frac{y_2^*}{y_1} = \frac{1}{2}(\sqrt{1+8F_1^2} - 1) \tag{2.1}$$

where,

$F_1 = \frac{V_1}{\sqrt{gy_1}}$ is Froude number of the supercritical flow

where,

y_1 is depth of the supercritical flow

V_1 is the average velocity of the supercritical flow

g is the acceleration of the gravity

y_2^* is depth of subcritical flow.

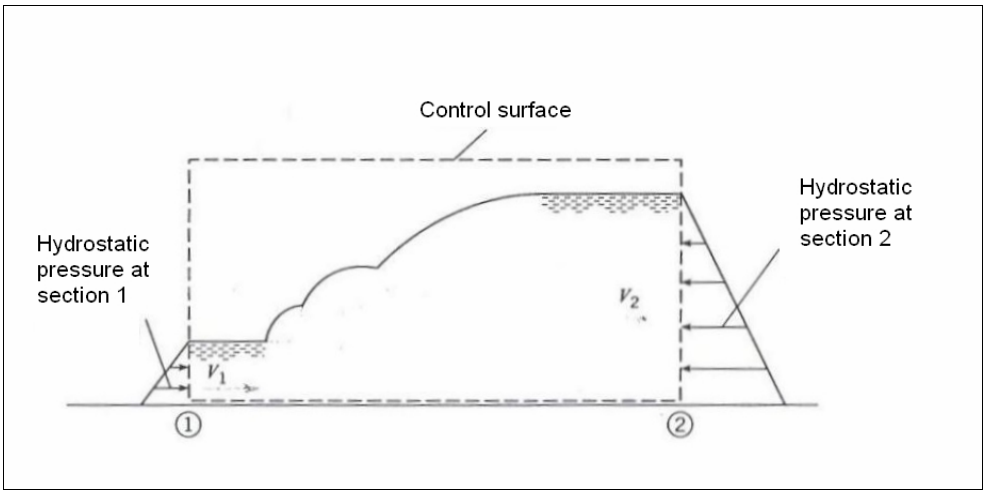

Figure 2.1: Control Volume for a Hydraulic Jump

If F_1>8.0, equation (2.1) can be approximated for purpose of quick estimation of the sequent depth ratio as *(Chow, 1959)*;

$$\frac{y_2^*}{y_1} \approx 1.41F_1 \tag{2.2}$$

Belanger equation does not include effect of friction along boundaries. The following momentum equation, which takes the friction into account, can be used to predict the sequent depth ratio more accurately than Belanger equation *(Ohtsu and Yasuda, 1990)*.

$$\left(\frac{y_2^*}{y_1}\right)^3 - \left[2F_1^2 + 1 - S_f\right]\left(\frac{y_2^*}{y_1}\right) + 2F_1^2 = 0 \qquad (2.3)$$

where, S_f is the integrated dimensionless bed shear force per unit width in the jump.

Hager and Bremen (1989) indicated that, for flows in which the incoming flow depth y_1 is small, there exists a significant scale effect on sequent depth ratio.

As stated in Hager and Bremen (1989), Harleman (1959) presented an equation for the ratio of sequent depths as;

$$F_1^2 = \frac{1}{2}\frac{Y[(Y+1)(Y-1)+\bar{S}]}{\beta_1 Y - (\beta_2 + J)} \qquad (2.4)$$

where

β_i is the momentum correction coefficient at section i, i=1,2

J is downstream turbulence-flux correction factor

Y is equal to sequent depth ratio y_2/ y_1

$\bar{S}$ is a non-dimensional bottom shear force and calculated as;

$$\bar{S} = \frac{2F_1^2}{V_1 R_1}\int_0^{L_J}\left(\frac{\partial \bar{u}}{\partial z}\right)_{Z=0} dx \qquad (2.5)$$

where

V_1 is incoming velocity of stream

Furthermore they investigated the variation of horizontal length scale with incoming Froude number and they expressed a formula to define horizontal length scale X, depending on incoming Froude number, as;

$$X = 5.08F_1 - 7.82 \tag{2.14}$$

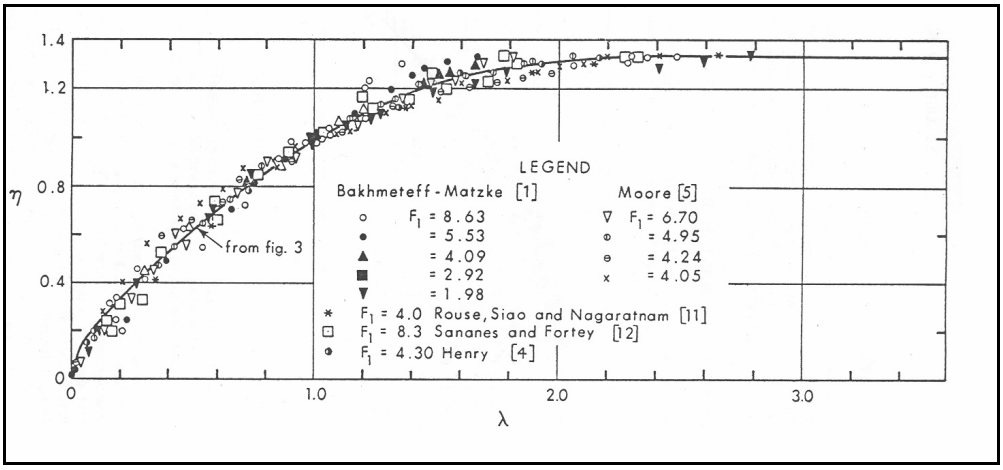

Figure 2.6: Non Dimensional Water Surface Profiles

(Rajaratnam and Subramanya, 1968)

2.1.5 Velocity Profile

Main factors which affect the velocity profile in jump body are shear stresses on solid boundaries and Reynolds stresses due to intense mixing between incoming supercritical stream and roller. Due to intense mixing, velocity profile in jump body is totally different from velocity profile of turbulent open channel flow. Shear force at the free surface of the jump affects only velocity profile in the roller.

When velocity profile of the hydraulic jump is investigated from the bottom to the free surface of the roller, it is observed that in the region, close to the channel bed, solid boundary is dominant on velocity profile, furthermore velocity profile is exactly same with the velocity profile of turbulent flows. This region, called boundary layer, has zero velocity at the bed and at the upper limit of this region, stream reaches to the highest velocity. In boundary layer region, velocity can be expressed as velocity defect law.

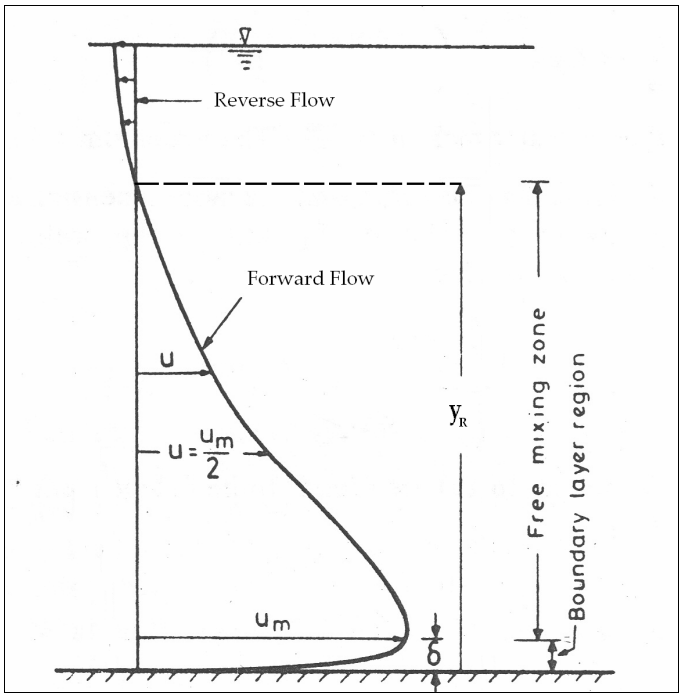

Fig.2.7: Velocity Profile in Hydraulic Jump *(Rajaratnam, 1965)*

The region between δ to the point y_R, where flow direction turns from forward to reverse and flow velocity is zero, is called as free mixing zone (Fig. 2.7). "In this zone, due to difference between the incoming stream velocity and velocity components of stationary surge in the direction of flow, velocity configuration of forward flow is similar to velocity profile of wall jets. In this region,

velocity profile can be studied by methods, used for analysis of wall jets *(Rajaratnam, 1965).”*

From the returning point to the free surface of roller, water flows in the opposite direction of the incoming stream.

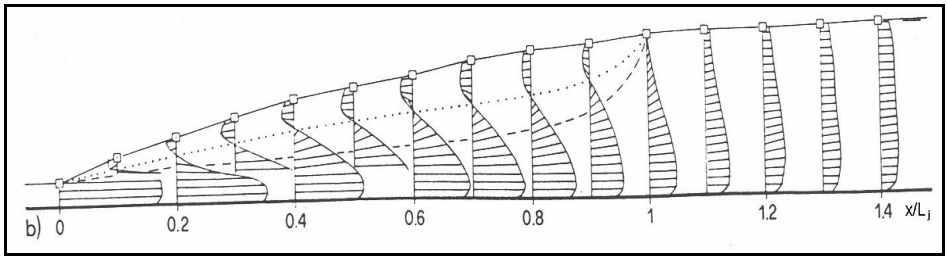

Figure 2.8: Velocity Profile along Jump *(Hager and Bremen, 1989)*

When velocity profile is examined along whole length of the roller, it is observed that reverse flow starts at the toe of the jump and at the end of the roller, reverse flow comes to an end as shown in Fig. 2.8 *(Hager and Bremen, 1989)*. Velocity profile along jump returns to the velocity profile of turbulent open channel flow practically at $x / L_J = 1.4$.

2.1.6 Classification of Jumps

The jump that will occur on a horizontal rectangular smooth channel has distinctive characteristics depending on the Froude number of incoming stream F_1. By increasing incoming Froude number F_1, the energy dissipation along hydraulic jump by turbulent mixing increases. Five different types of jump had been defined for horizontal rectangular smooth channels depending on

incoming Froude number of the stream, however basic parameter of these classification is founded on shapes of jumps.

The ranges of Froude number given below depend on local conditions and are not clear-cut, so the possibility of change of ranges must be taken into account in design considerations.

Undular Jump; $1<F_1\leq1.7$: The water surface is undulating with a very small ripple on the surface. The sequent depth ratio is very small and E_L/E_1 is practically zero.

Weak Jump; $1.7<F_1\leq2.5$: The surface roller makes its appearance at $F_1 \approx 1.7$ and flow phenomena for this range of Froude numbers in pre-jump stage. The energy dissipation is very small, E_L/E_1 changes from 5% at $F_1 = 1.7$ to 18% at $F_1 = 2.5$ approximately.

Oscillating Jump; $2.5<F_1\leq4.7$: For these range of Froude numbers, a true hydraulic jump does not fully develop. Jump is instable, oscillates in a random manner and these oscillations produce large surface waves in irregular period. Energy dissipation is change from 18% to 45 % by the increase in Froude number.

Steady Jump; $4.5<F_1\leq9$: True hydraulic jump form for Froude numbers greater than 4.5. Position of steady jump is the least sensitive type to fluctuations in the tailwater elevation. The relative energy loss E_L/E_1 changes between 45% to 70%.

Strong or Choppy Jump; $9<F_1$: For hydraulic Jumps in which the upstream Froude number is greater than 9, the water surface profile along the jump and downstream the jump are rough and wavy. Relative energy loss is greater than 70% and up to 85%.

2.1.7 Position of the Jump

A hydraulic jump is formed whenever the momentum equation is satisfied between the supercritical and subcritical parts of the stream. In other words, if the initial depth y_1, the sequent depth y_2^* and the approaching Froude number, F_1 satisfies equation (2.1) in smooth rectangular channel, the hydraulic jump will occur.

2.2 Hydraulic Jumps on Rough Beds

Turbulent flow over a rough surface is an important problem and it has been subject of diverse fields. The flow over a surface with transverse, rectangular roughness elements often used as a simple model to study roughness effects on friction factor, heat transfer, and hydraulic jump.

On the other hand, when water is used to examine the effect of roughness on turbulent flow, roughness elements are subjected to cavitation if flow velocity is high.

To avoid cavitation, roughness elements should be installed to the stream bed with such an arrangement that, the crest of roughness elements will be at the same level of upstream bed. Hence, the roughness elements would not be protruding into the flow and subjected lower intensity of cavitation when compared with protruding roughness.

Ead and Rajaratnam (2002) and *Ayanlar (2004)* examined the reduction of tail water depth due to corrugated beds experimentally. Reduction of tail water depth was found about 25% by *Ead and Rajaratnam (2002)* and 20% by

Ayanlar (2004). It is an important point that efficiency of corrugated beds are higher than USBR stilling basins Type II and Type III when reduction of tail water depths are compared *Ayanlar (2004)*. Furthermore it was observed that the lengths of jumps on corrugated beds are approximately one-half of those of the classical; shorter than USBR Type II basin and only slightly longer than Type III.

Early experimental works have shown that the pitch ratio w/z is an important parameter for flows on roughened beds where w is the distance between two roughness elements and z is the height of roughness element *(Cui at al., 2003)*. For d-type roughness, roughness elements so closely spaced that, crests of the ribs do not penetrate into flow and the effect of roughness elements on friction and eddy formation is negligible. A vortex fills the cavity between the two ribs and effects of a pitch on bulk flow look like as the effect of a cavity on bulk flow for this range of pitch ratio or this type of roughness *(Cui at al., 2003)*.

If the pitch ratio is equal to 4, it is known as intermediate roughness, the length of vortex formed in the cavity is equal to the length of the gap between roughness elements. "This vortex prevents the outer flow from attaching to the channel bed and streamlines above the pitch nearly parallel except near the roughness element *(Cui at al., 2003)"*.

If the pitch ratio is greater than 4, it is called as k-type roughness, vortex formed in the cavity is smaller than pitch, and hence outer flow attaches to the channel bed. Roughness elements penetrate into flow and friction factor depends on the size of roughness elements. Flow structures in the gaps for these three types of pitch ratios are shown in Fig. 2.9.

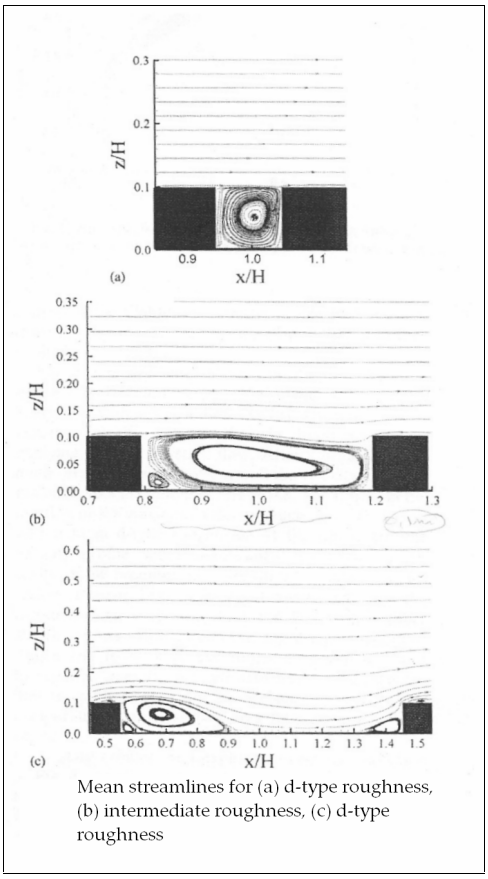

Fig.2.9: Flow Structures for Different Pitch Ratios *(Cui at al., 2003)*

Vortexes formed for k-type and intermediate type roughness increase turbulent intensities in the plane of crests of roughness elements, hence also increase Reynolds shear stresses.

Furthermore the pressure drags on the roughness elements much higher than friction drag of smooth channel and increases the resistance to the flow *(Cui at al(2003).* indicated that for k-type roughness, the resistance to the flow is 6 times higher than resistance of a smooth channel, whereas for the intermediate type roughness this ratio is about 4.6.

Using roughness elements at the bottom of the flow causes an increase in resistance to the flow, hence increase in amount of kinetic energy converted into the heat. In this manner, the use of roughened beds at stilling basins where hydraulic jumps occur increases amount of energy dissipated along jump.

In smooth channels, the dissipation of energy occurs only along roller and some how downstream of the roller. Any change in tailwater depth changes the position of the jump significantly in smooth beds. On the other hand, if the channel is roughened, the resistance of flow is greater than that of smooth surfaces. Hence the position of the jump on rough beds is less sensitive to the change in tailwater depths when compared with smooth surfaces.

2.2.1 Definitions and Related Parameters Used in the Present Study

The definitions and related parameters used in the present study are shown in Fig. 2.10.

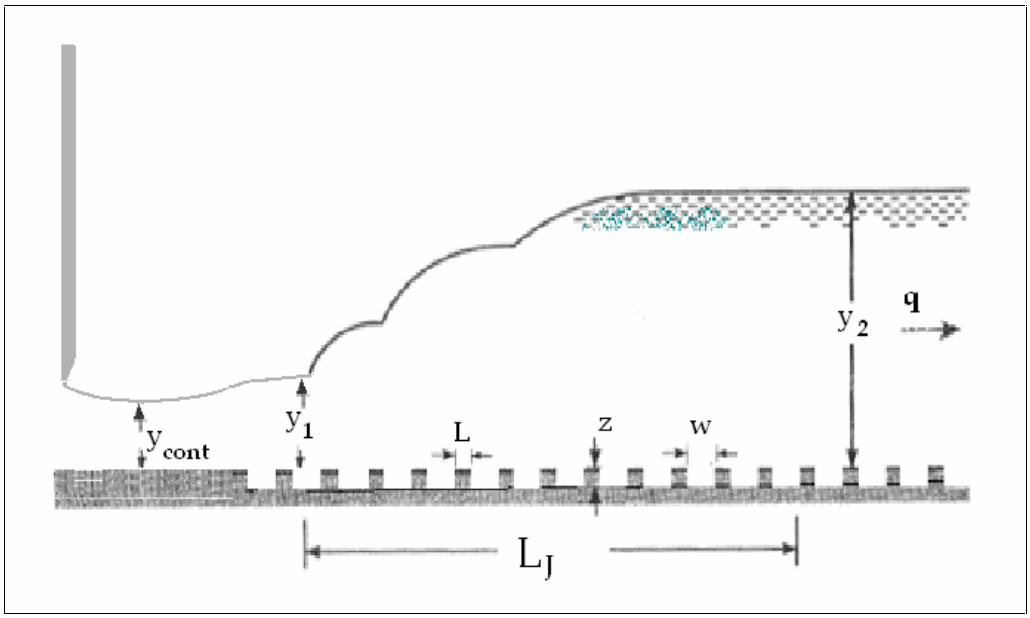

Figure 2.10: Related Parameters of Hydraulic Jump on Rough Bed

The tailwater depth, y_2 and the length L_J, for the hydraulic jump on a rough bed may be a function of the following parameters.

$$y_2 = f_1(y_1, q, L, z, w, g, \rho, \upsilon) \tag{2.15}$$

$$L_J = f_2(y_1, q, L, z, w, g, \rho, \upsilon) \tag{2.16}$$

where,

y_1 is the incoming flow depth which is measured from the crests of roughness elements to the water surface,
y_2 is the tailwater depth which is measured from the crests of roughness elements to the water surface,
q is the discharge in per unit width of the flow
L_J is the length of the jump
z is the height of the roughness element
L is the length of roughness element
w is the distance between two roughness element
g is the acceleration of gravity
ρ is the mass density of water,
υ is the kinematic viscosity of water

To perform the dimensional analysis for the problem, y_1, q and ρ is chosen as the repeating variables, and the following dimensionless parameters may be found;

$$\frac{y_2}{y_1} = f_3\left(\frac{q^2}{g y_1^3}, \frac{L}{y_1}, \frac{z}{y_1}, \frac{w}{y_1}, \frac{q}{\upsilon}\right) \tag{2.17}$$

$$\frac{L_J}{y_1} = f_4\left(\frac{q^2}{gy_1^3}, \frac{L}{y_1}, \frac{z}{y_1}, \frac{w}{y_1}, \frac{q}{\upsilon}\right) \tag{2.18}$$

To compare the length of the jump with that of on smooth bed, y_1 is replaced by y_2^*, which is the conjugate depth of y_1 corresponding to the hydraulic jump on a smooth bed *(Ead and Rajaratnam, 2002)*. Viscous forces are not significant with respect to the gravitational force, so Reynolds number, q/υ can be neglected *(Rajaratnam, 1965)*, and the first term is equal to incoming Froude number. The second, the third and the fourth terms may be combined as the pitch ratio w / z, and the length ratio w / L, hence equations (2.17) and (2.18) may be rewritten as;

$$\frac{y_2}{y_1} = f_5\left(F_1, \frac{w}{z}, \frac{w}{L}\right) \tag{2.19}$$

Similarly, for the length of the jump the following relationship may be obtained.

$$\frac{L_j}{y_2^*} = f_6\left(F_1, \frac{w}{z}, \frac{w}{L}\right) \tag{2.20}$$

CHAPTER III

EXPERIMENTAL APPARATUS AND EXPERIMENTS

3.1 Description of the Experimental Setup

Experimental study was conducted in a horizontal, rectangular open channel; 25.3 cm wide, 43.2 cm deep and 1000 cm long which is schematically represented in Fig. 3.1. The channel was made of concrete and fiberglass such that the wall of the middle section, which was 364 cm long, was made of fiberglass and the remaining parts at the entry and outlet of the channel were made of concrete. Roughness elements were placed in fiberglass section of the channel. Tailwater depth was controlled by an adjustable weir placed at the end of the channel.

Supercritical uniform stream obtained by an adjustable sluice gate at the entrance of the channel was not appropriate to obtain large Froude numbers. The maximum Froude number obtained by using sluice gate was 4.2. To handle this problem, a pressure tank was installed into inflow channel reach and range of Froude numbers were increased up to 17. Setup of the pressure tank and view of the pressure tank is shown in Fig. 3.2 and Fig. 3.3, respectively.

Water was supplied to pressure tank from a constant head tank through an 18 cm pipe which is regulated by a valve. Water issuing out from the downstream weir was collected in a basin. This basin was connected to a return channel, 25

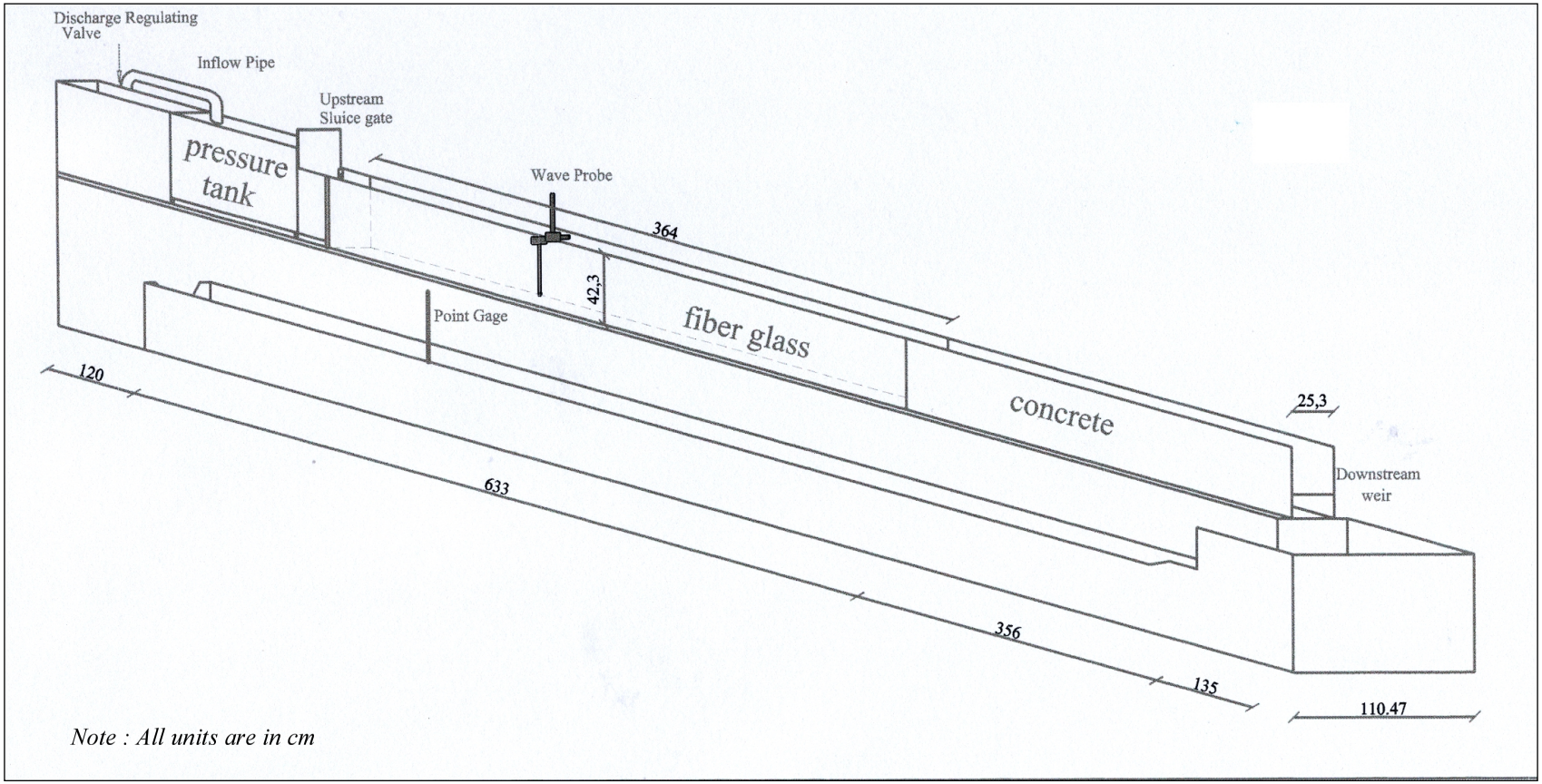

Figure 3.1: Schematic Representation of Experimental Setup

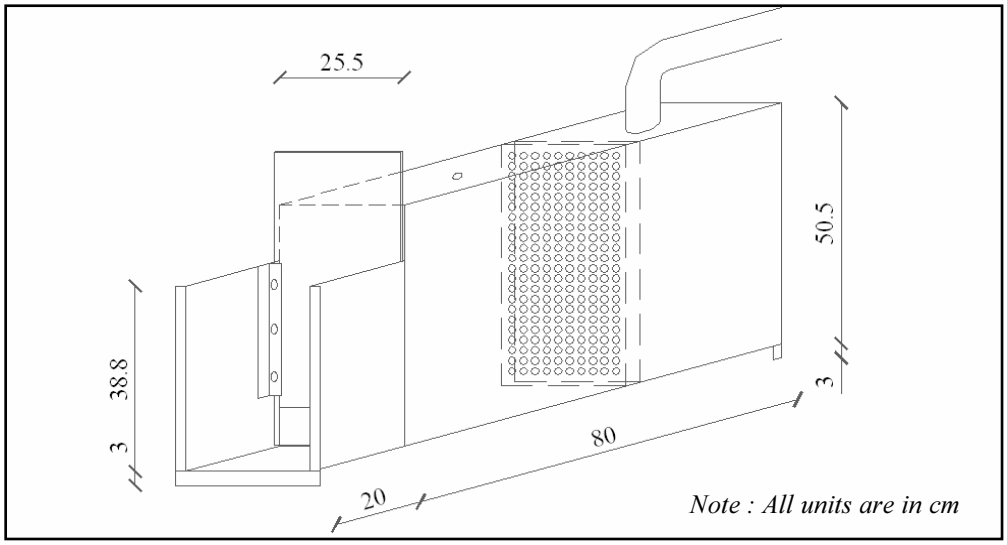

Figure 3.2: Dimensions of Pressure Tank

Figure 3.3: General View of Pressure Tank

cm wide, 40 cm deep and 745 cm long. Discharge measurements were made by a triangular weir, with 30˚ notch angle, placed at the end of the return channel.

Pressure tank was designed such that the bed of tank outlet would be 3 cm higher than channel bed. The reason was to let the crests of roughness elements to have the same level of upstream bed carrying the supercritical stream.

3.2 Description of Roughness Elements

Three different sizes of roughness elements, produced from fiberglass, were used in the experiments. The heights of roughness elements were 0,6 cm, 1 cm and 2 cm. All roughness elements had 25 cm width and 1 cm length. To arrange wavelength for each roughened bed and to satisfy the condition that the crests of roughness elements to have the same level of upstream bed, three different fiberglass sheets were used. Heights of fiberglass sheets were 2.4 cm, 2 cm and 1 cm; all sheets had 25 cm width and 300 cm length.

Roughness elements could be screwed into fiberglass sheets in such a way that the wavelength, (w+L), of roughened beds would be 5 cm, 10 cm, 15 cm and 20 cm. Roughness elements with 0.6 cm height were screwed into sheet with 2.4 cm height; roughness element with 1.0 cm height was screwed into sheet with 2.0 cm height and roughness element with 2.0 cm height screwed into sheet with 1.0 cm height. Four types of roughness element arrangements are shown in Fig. 3.4.

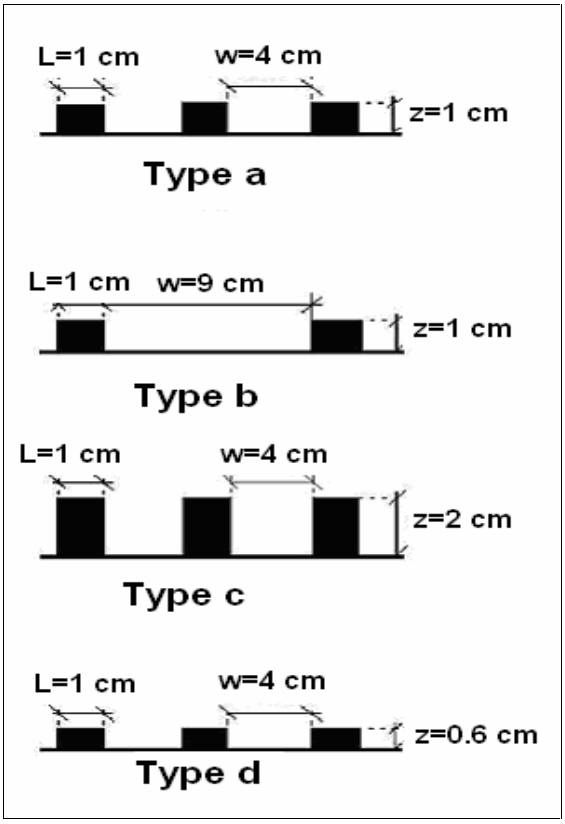

Figure 3.4: Types of Roughness

3.3 Calibration of the Triangular Weir

Before the hydraulic jump experiments, the calibration of the triangular weir has been done by measuring the flow velocity in the channel. The measured velocities were integrated numerically to obtain the discharge (See Appendix C). Results were compared with the discharge equation of triangular weir, Eq. (3.1), to find the proper contraction coefficient C_C of the weir.

$$Q = \frac{8}{15} C_c \tan\frac{\alpha}{2} \sqrt{2g} H^{\frac{5}{2}} \quad \text{.....(3.1)}$$

where,

Q is the volumetric discharge

Cc is the contraction coefficient for triangular weir

α is the notch angle of triangular weir

g is the acceleration of gravity

H is the head measured on the triangular weir.

The contraction coefficient C_C was found to be C_C=0.58. The result of the calibration curve is shown in Fig. 3.5.

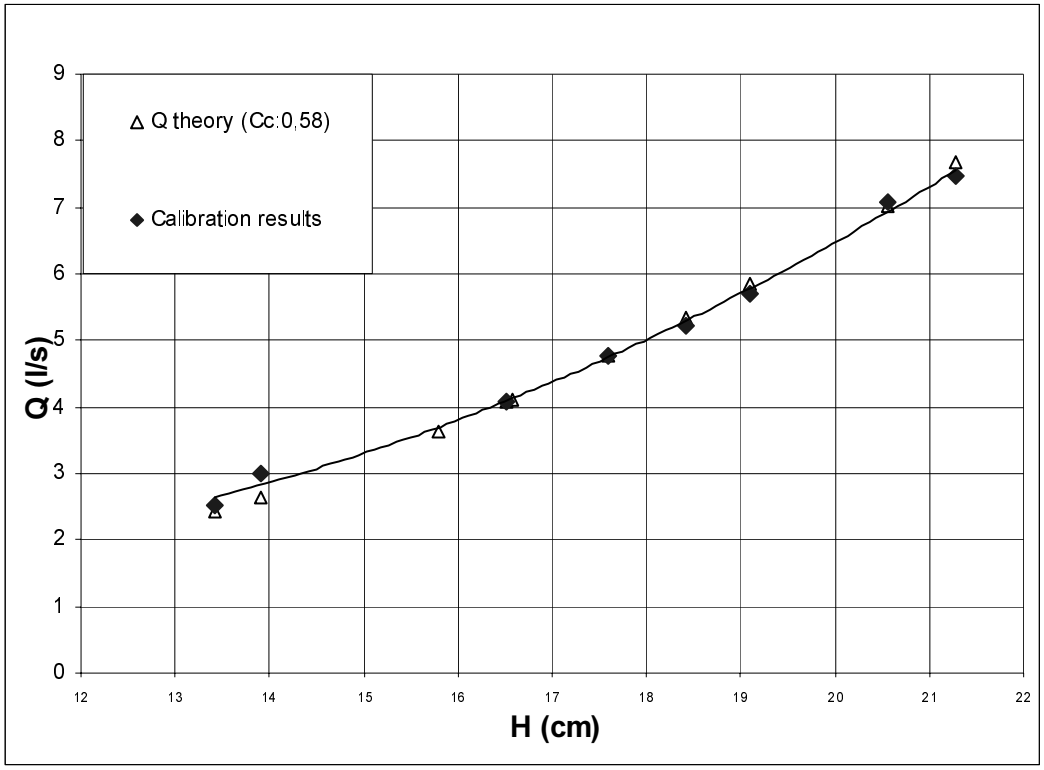

Figure 3.5: Head vs. Discharge Curve of Triangular Weir

3.4 Measurements

In every set of experiments, H, head on V-notch; y_1, the water depth of incoming flow just before jump; y_2, the subcritical tailwater depth; X_J the starting point of jump; L_J, length of jump and water surface profile of jump, were measured.

Flow discharge is calculated according to equation Eq. (3.1), with contraction coefficient C_C = 0.58. The water depths y_1 and y_2 were measured by a point gage which has sensitivity of 0.1 mm.

Water surface profile was measured by the help of H.R. Wallingford Wave Probe Monitor (Item Code CLE3 C30) shown in Fig. 3.6. Wave Probe was fixed to an apparatus, which can move along and across the channel. Measurements were done for 5 cm intervals along the flow direction and position of apparatus was fixed to take measurements in the middle of the channel.

Wave probe was connected to Wave Probe Monitor and it was linked to WPA CQ95 pointer. Wave Probe Monitor was used at 50 mV/cm sensitivity and pointer was used at 10 mm/sec speed. Pointer prints water depth into roll of millimeter scaled paper according to level of water, above the bottom of the wave probe.

While performing experiments, the probe was moved 5 cm downstream at 5 sec. time intervals in the jump body to satisfy equality of length scales of the pointer and the jump. Printed profile of the hydraulic jump on millimeter scaled paper read manually by taking averages at each 5 cm interval. From the printed profile of the hydraulic jump, the water depth y_1 of incoming flow and tailwater depth y_2 could also be obtained.

Figure 3.6: View of Wave Probe Monitor and Plotter

Figure 3.7: View of Wave Probe

To use the wave probe, the probe monitor and the pointer, the calibration of the probe had to be done before each experiment. The calibration of the probe was made by sinking the wave probe into calm water with known depths. Printed values on paper for known depths are calculated manually and calibration curve was obtained. Calibration curve for experiments 1-22 is shown in Fig. 3.8.

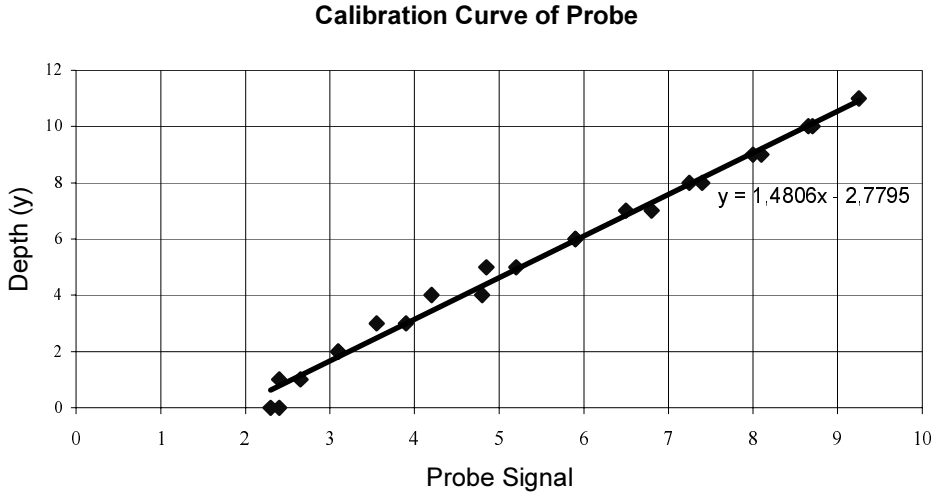

Figure 3.8: Calibration Curve of Probe

The starting point of jump, X_J, was measured by tape. The distance from the beginning of the channel bed to the section, where water surface was started to fluctuate, was defined as starting point of jump. From printed surface profiles, starting point of the hydraulic jump was observed practically by the investigation of the fluctuations.

The length of jump was obtained by taking differences between the starting point of the jump and the end of the jump, which were measured by tape. The

point, where water surface is essentially level was defined as the end of jump. The end of jump could also be observed practically from printed surface profiles.

Furthermore, fiberglass sidewalls of the channel had been scaled. High resolution photographs (2048×1536 pxs) were taken for each profile of the jump. Before each photograph was taken, potassium permanganate was spilled into to channel entrance, hence roller of jump was observed more easily. The water depth y_1, y_2 and the profile of the hydraulic jump were also investigated by high resolution photographs.

The Froude number range of experiments is between $7.4 \leq F_1 \leq 16.6$, and w/z, pitch ratio changes between $2 \leq w/z \leq 9$ in the experimental study. Furthermore, the effect of length ratio, w/L, on jump properties was examined for two different values of length ratio, 4 and 9.

CHAPTER IV

RESULTS AND DISCUSSION OF RESULTS

4.1 Observations

In this study, data of 81 sets of experiments were used to express the effect of rough beds on the hydraulic jump properties. Initial experimental setup including an adjustable sluice gate was used, however experimental studies on this setup had shown that initial setup would not satisfy scope of present study. A hydraulic jump, produced in initial setup is shown in Fig. 4.1.

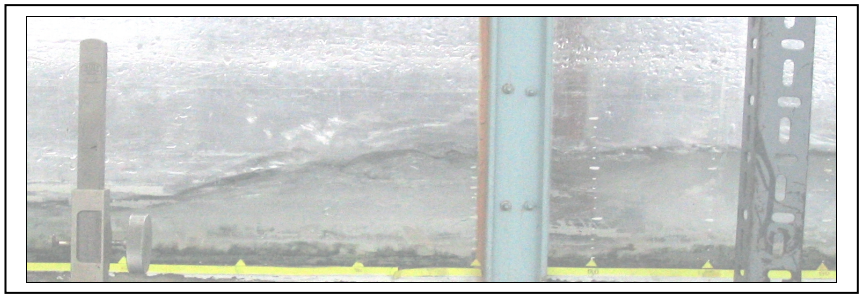

Figure 4.1: A Hydraulic Jump from Initial Experimental Setup

Along experimental studies, different roughness types, length ratios and pitch ratios were used to investigate the effect of roughness on hydraulic jump properties. At the beginning the target of the study was to investigate the effect

of different length and pitch ratios on jump properties. On the other hand for the length ratios 14 and 19, the first roughness element disturbs flow as shown in Fig 4.2, and it was decided that these roughness arrangements could not be used in the study.

Figure 4.2: Effect of Pitch Ratios 14 and 19 on Flow Structure

A close view of the first roughness element, which is dominant on flow structure, is given in Fig 4.3.

Figure 4.3: Effect of First Roughness Element on Flow Structure

There are different types of hydraulic jumps as mentioned in Sec. (2.1.7). However, only steady and strong jumps were investigated in this study.

Photographs of some observed steady and strong jumps are given in Fig. 4.4 and Fig. 4.5, respectively.

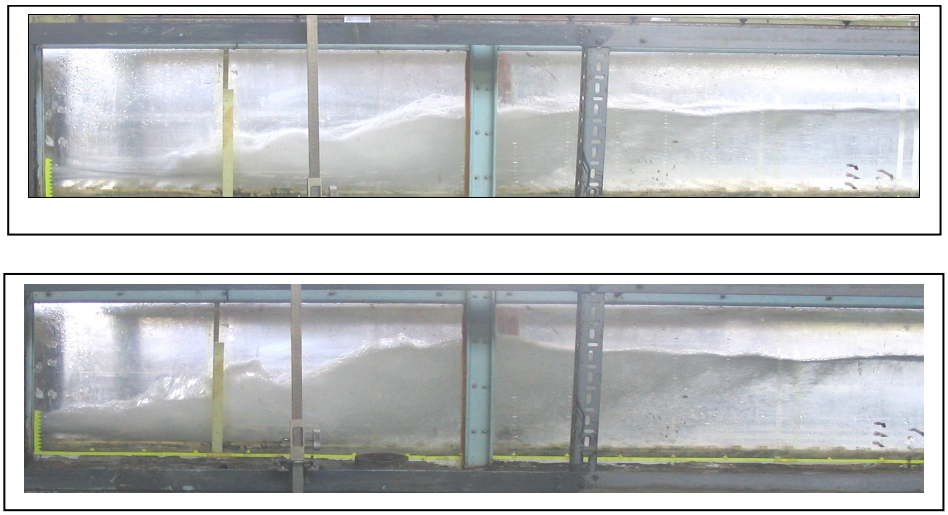

Figure 4.4: Steady Jumps

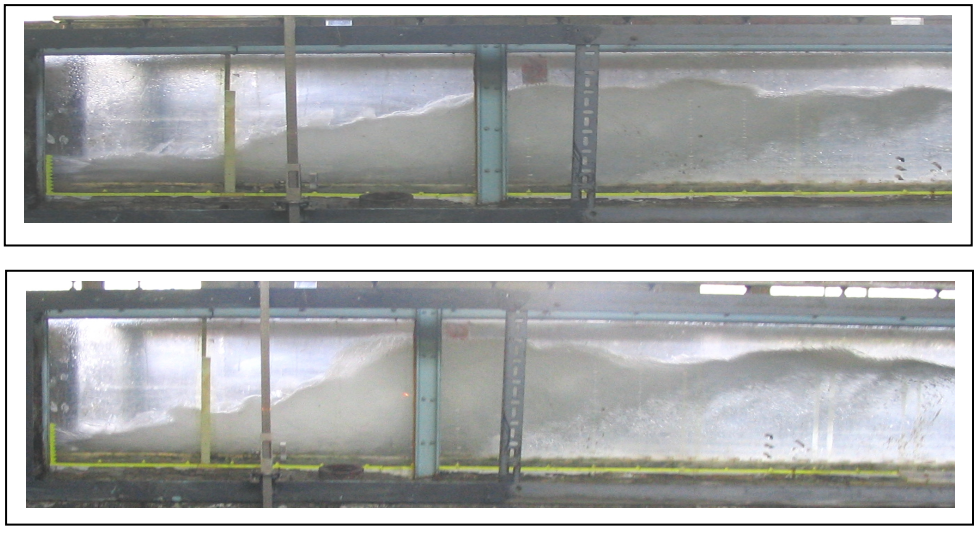

Figure 4.5: Strong or Choppy Jumps

4.2 Energy Loss along Channel

Effect of pitch ratio on flow structure examined in Sec. (2.2) and flow structures was illustrated in Fig. 2.12 It is shown that depending on the pitch ratio, structure of vortex between two roughness elements and the effects of the vortex on bulk flow change abruptly.

The first roughness element was placed 20 cm far from the gate and front face of the first roughness element was taken as starting point of the x axis. Four different types of pitch ratio, 2, 4, 6 and 9 and two different values of length ratio, w/L, 4 and 9 were used in the experiments.

The percent specific energy loss of the flow from vena contracta to the point where jump starts i.e. between sections (1) and (2) in Fig. 2.10, is shown in Fig. 4.6.a and 4.6.b for length ratios w / L = 4 and w / L = 9 respectively. Flow depth at vena contracta calculated by Eq.(4.1.) *(Chow, 1959)*.

$$y_{CONT.} = 0.61 \cdot a \tag{4.1}$$

Where, y_{CONT} is the flow depth at vena contracta and a is the gate opening.

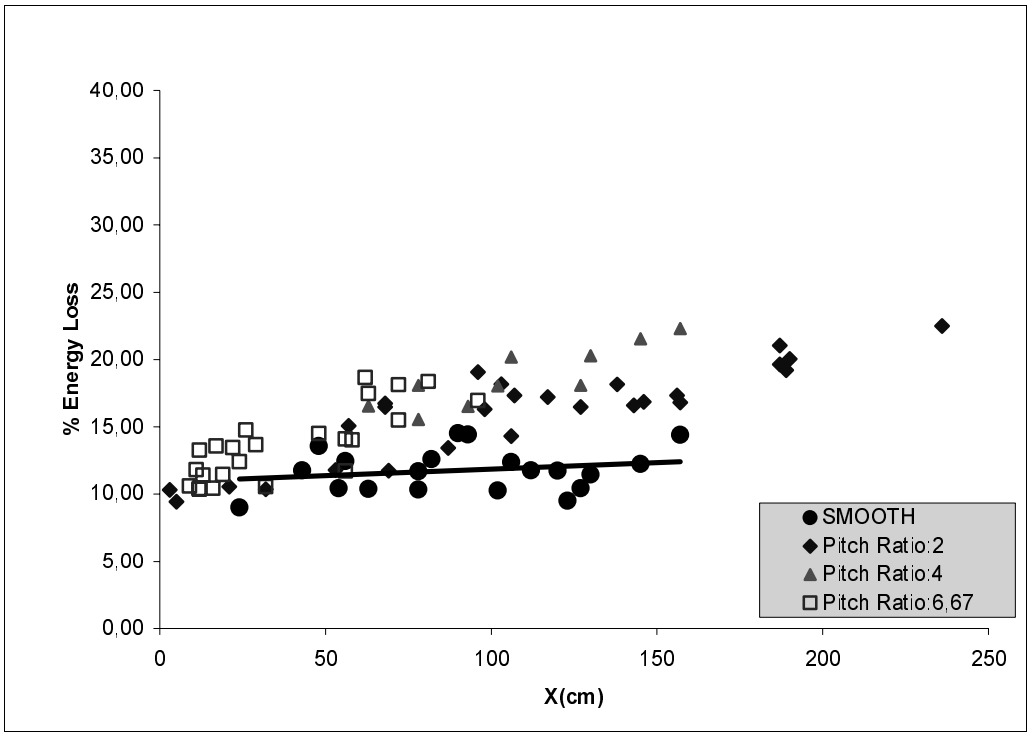

Figure 4. 6. a: Percent Energy Loss for Length Ratio w / L = 4

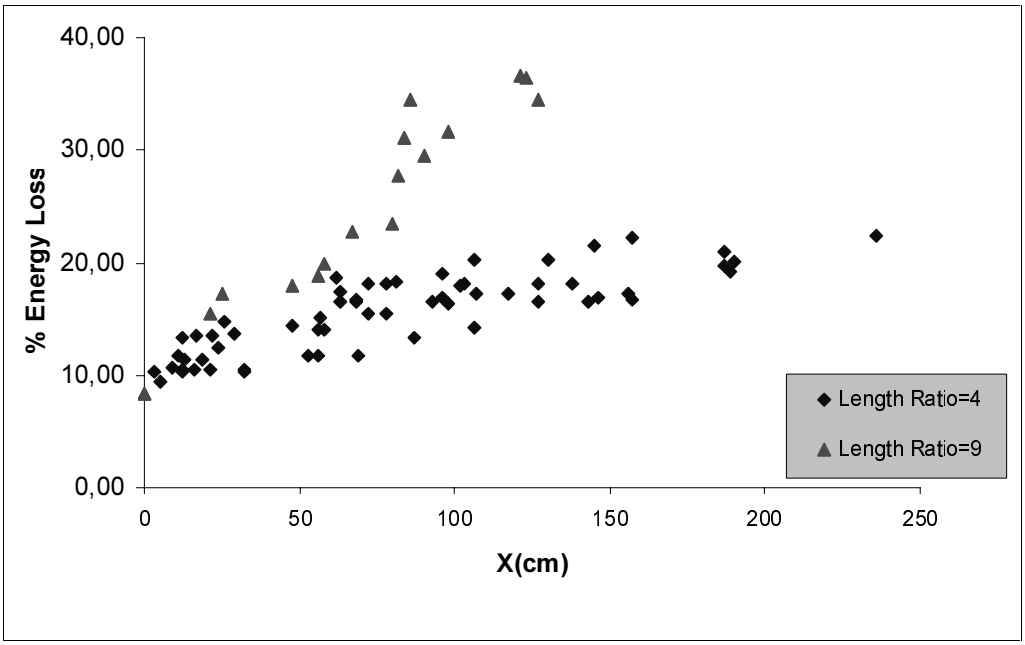

Figure 4. 6. b: Percent Energy Loss in the Channel for Length Ratios w / L = 9 and w / L = 4

In Fig. 4.6.a., the energy loss between the vena contracta and the toe of the jump for length ratios w / L = 4 and for smooth bed are shown. Fig. 4.6.a shows that the percent energy loss for rough bed is higher than the smooth bed as expected. Smooth bed data show that the percent energy loss is about 10%, and 15% for w / L = 4 for a range of pitch ratio of $2 \leq w / z \leq 6.67$. However, for a constant length ratio of w / L = 4, the percent energy loss does not show any significant variation with the pitch ratio w / z. Therefore in Fig. 4.6.b., the percent energy loss for length ratio w / L = 9 and w/L = 4 are given to show the effect of length ratio.

Fig. 4.6.b. shows that for w / L =9 and w / z =9, there is an appreciable increase and different trend for the percent energy loss for w / L =9 and w / L = 4. Therefore, we may conclude that, it is the length ratio w / L which is more effective on the energy loss rather than the pitch ratio w / z.

4.3 Depth Ratio

According to the dimensional analysis performed in Sec. (2.2.1), the pitch ratio, w/z may affect the depth ratio y_2/y_1. Furthermore, length ratio may also have effect on depth ratio.

To determine the effect of the pitch ratio and the effect of the length ratio on the tail water depth ratio, y_2/y_1 values versus F_1 were sketched separately in Fig. 4.7.

Fig. 4.7 shows that the roughness reduces the required tail water depth for a given upstream condition, y_1 and F_1, when compared with the results of the hydraulic jumps on smooth bed. It is also realized that effect of different pitch

ratios and length ratios on depth ratio along hydraulic jump is practically the same and the effect of pitch and length ratios are not important on depth ratio of the hydraulic jump, provided that the vortex is confined between the roughness cavity.

The effect of different roughness types on depth ratio of hydraulic jump is shown in Fig. 4.8. *Ead and Rajaratnam (2002*) and *Ayanlar (2004)* had studied the corrugated beds. The data of these studies and the depth ratio for smooth beds obtained from Eq. 2.1. are shown with the data obtained in the present study in Fig. 4.8.

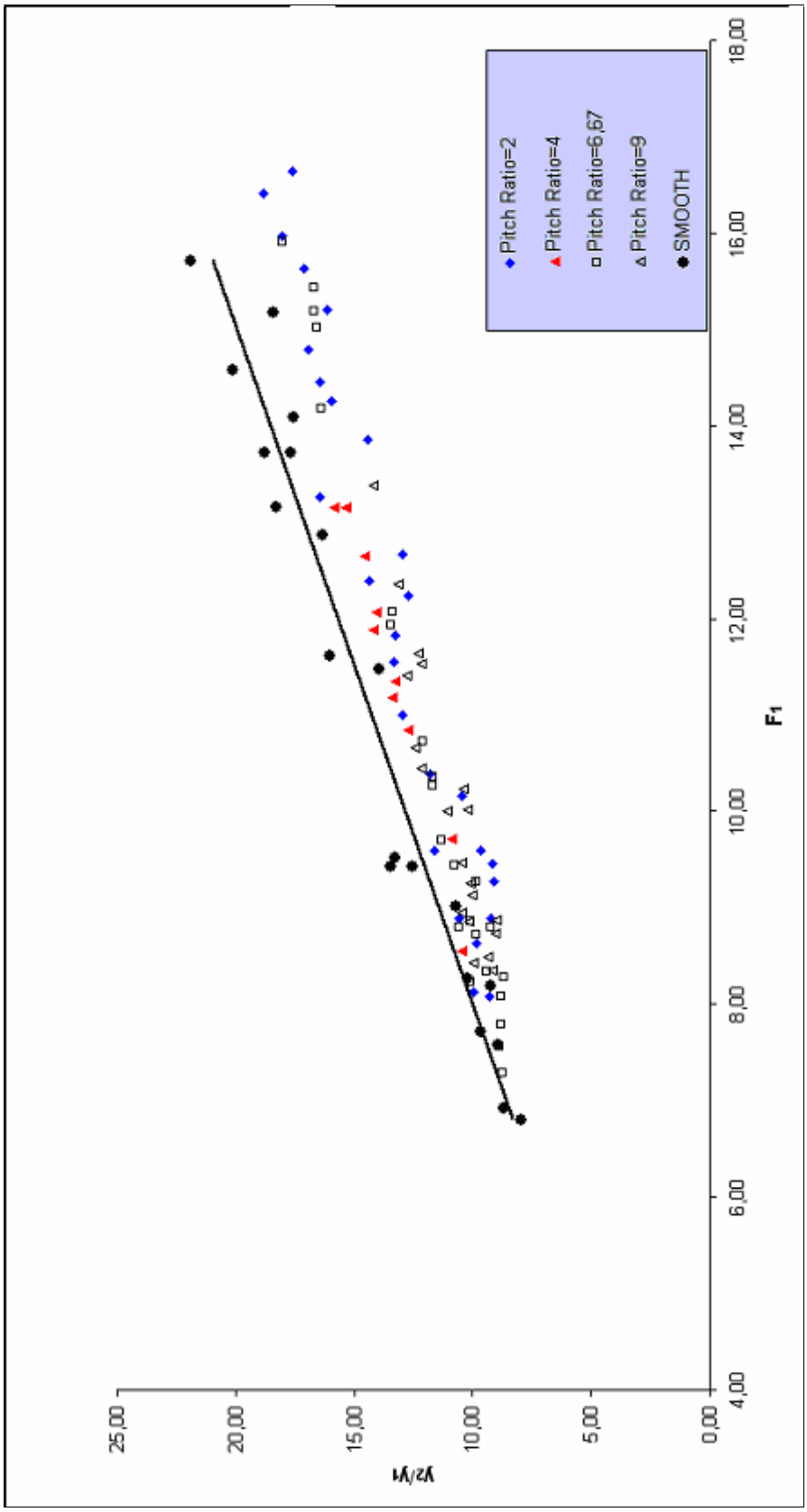

Figure 4. 7: Tail Water Depth – Supercritical Depth Ratio versus Upstream Froude Number

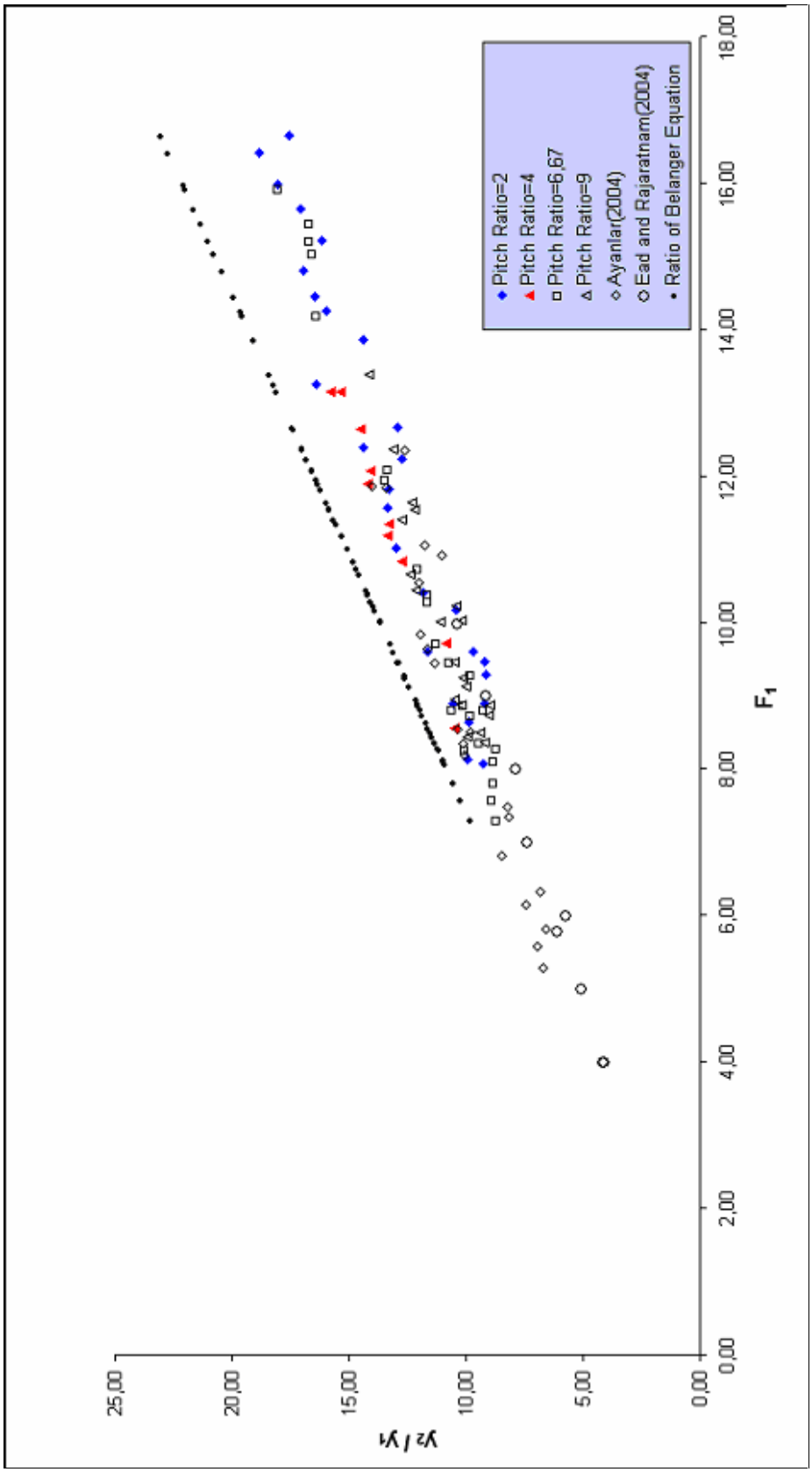

Figure 4.8: Tail Water Depth – Supercritical Depth Ratio for Different Roughness Types

Fig. 4.8 shows that rough beds decrease depth ratio compared with jumps on smooth beds. On the other hand, it is observed that corrugated beds and rough beds with prismatic roughness elements have the same effect on tailwater depth. This may be due to the fact that in both types of roughnesses the vortex formed is confined between cavities of roughnesses.

For the pitch ratio 9, it is expected that the effect of the roughness on depth ratio should be different from other pitch ratios according to Sec. (2.2). However, the different behavior of flow structure for this pitch ratio shows its difference at energy loss along channel as stated in Sec.(4.2).

4.4 Reduction in Tail Water Depth

To compare the measured tailwater depths with the conjugate depths of the incoming flow, a simple ratio, D was introduced as;

$$D = \frac{y_2^* - y_2}{y_2^*} \tag{4.2}$$

where, y_2^* is the sequent depth of y_1 for corresponding classical jump on a smooth bed.

This ratio was called as the tailwater reduction factor and used to express experimental results in *Ead and Rajaratnam(2002)* and *Ayanlar(2004).* The variation of D with F_1 is shown in Fig 4.9 for different pitch ratios.

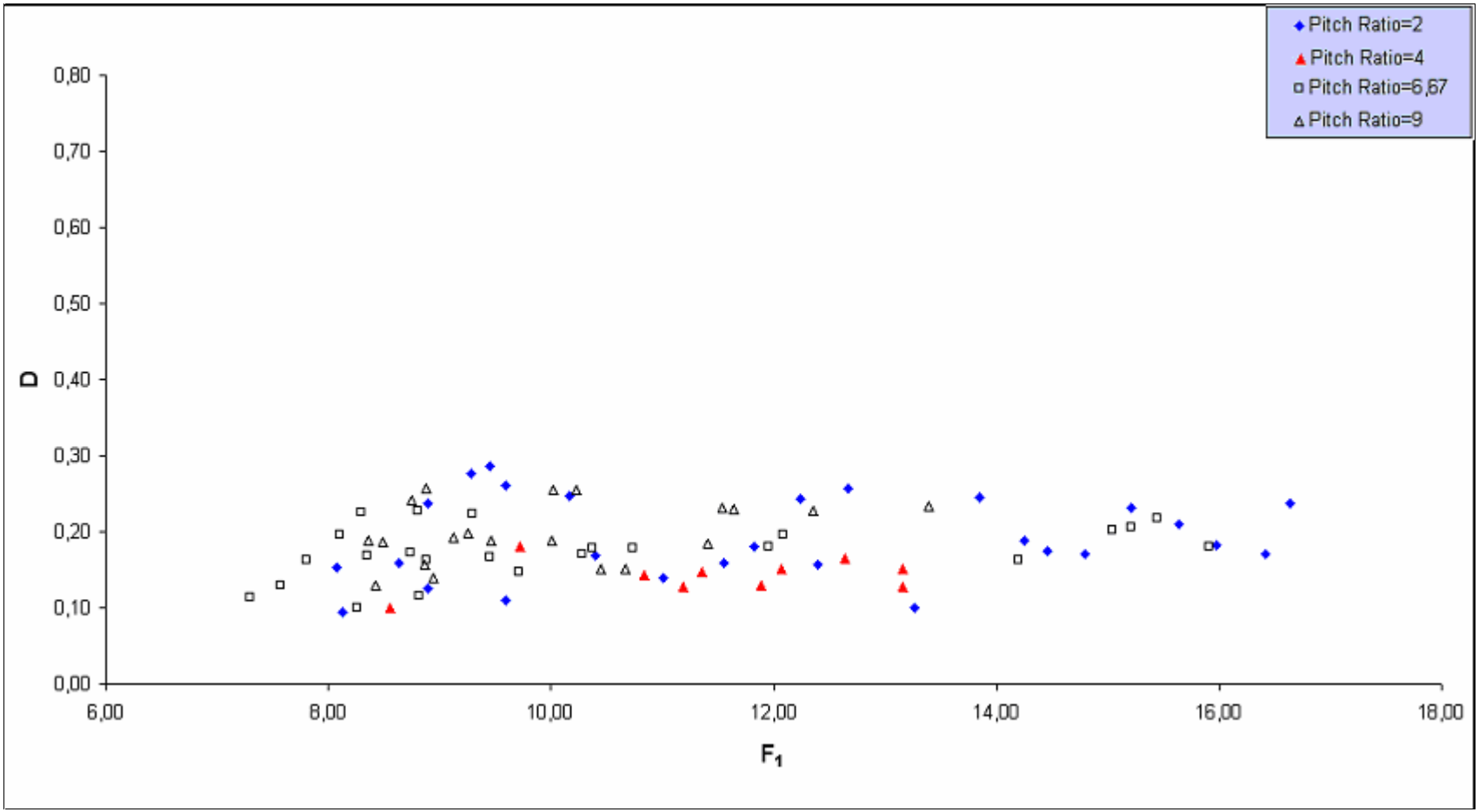

Figure 4. 9: Reduction in Tailwater Depth in the Jumps for Different Pitch Ratios

Fig.4.9 shows that an average reduction factor of 0,2 may be considered for the ranges of experiments, pitch ratios from 2 to 9 and incoming Froude number in the range of $7.3 \leq F_1 \leq 16.50$ with prismatic roughness.

To compare roughened beds with corrugated beds, the data of *Ead and Rajaratnam (2003)* and *Ayanlar (2004)* are shown in Fig. 4.10, together with the data obtained in the present study.

Fig. 4.10 shows that either on corrugated or roughened beds, tailwater depth decreases when compared with jumps on smooth beds. The reduction of tailwater depth changes between 10% and 30%; however it tends to be equal at a constant value of 19~20%. Jump height is an important design criterion for the stilling basins; hence use of roughness seems to be affective to obtain more economical stilling basin design compared to that on smooth beds.

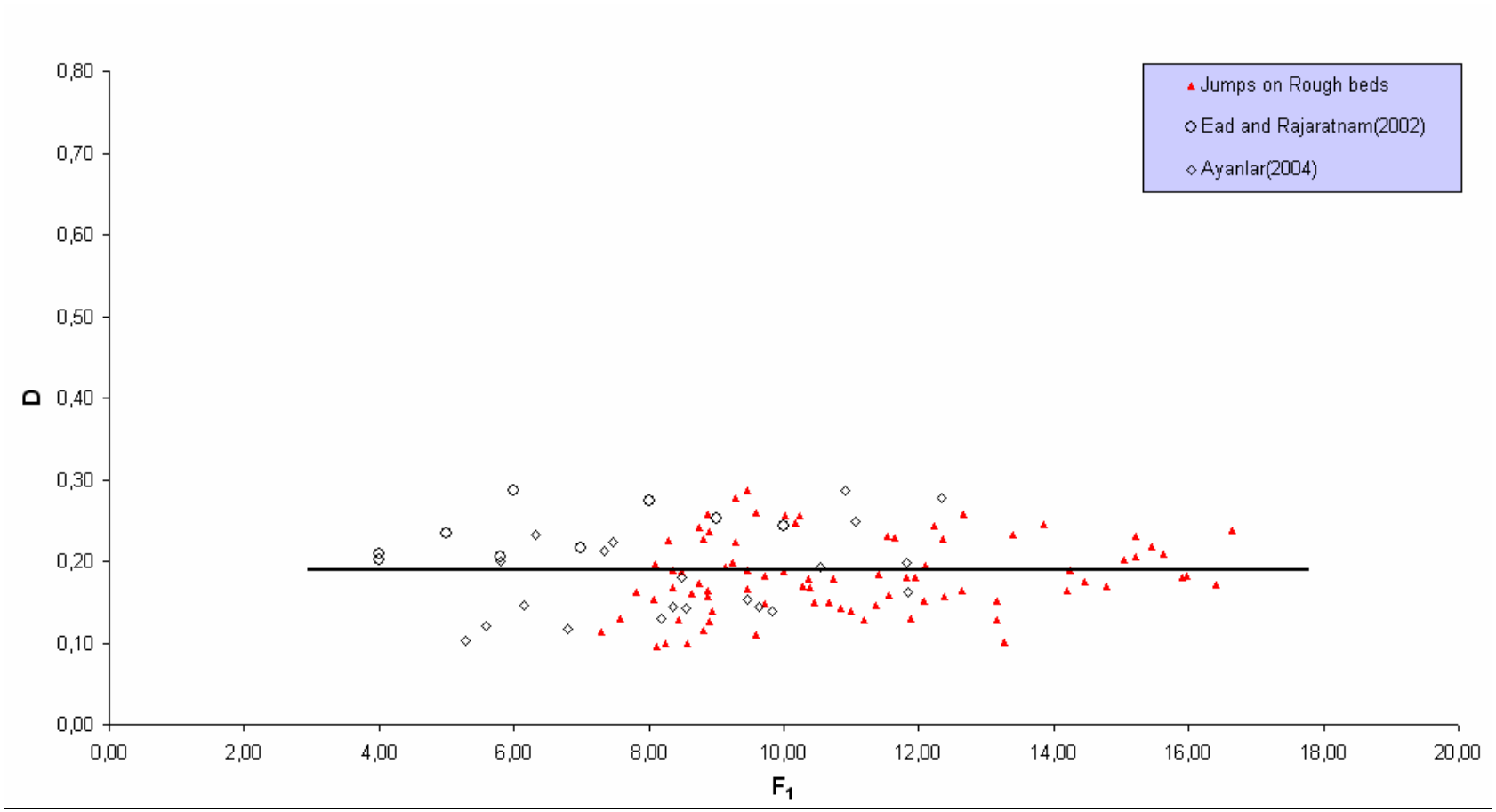

Figure 4. 10: Reduction in Tailwater Depth in Jumps for Different Roughness Types

4.5 Length of Hydraulic Jump

To determine the effect of roughness on the length of jump, the length of jumps measured in the experiments are non-dimensioned by dividing by y_2^*. Where y_2^* is conjugate depth of a simple hydraulic jump for a given upstream condition, y_1 and F_1.

L_j/y_2^* versus F_1 values of the experiments with different pitch ratios are plotted in Fig. 4.11 therefore the effect of different types of roughness on length of jump may be compared. L_j/y_2^* versus F_1 values for smooth case and *USBR (1955)* data also plotted in Fig. 4.11.

In Fig 4.12, the comparison of the effect of different length ratios on the length of hydraulic jump is shown.

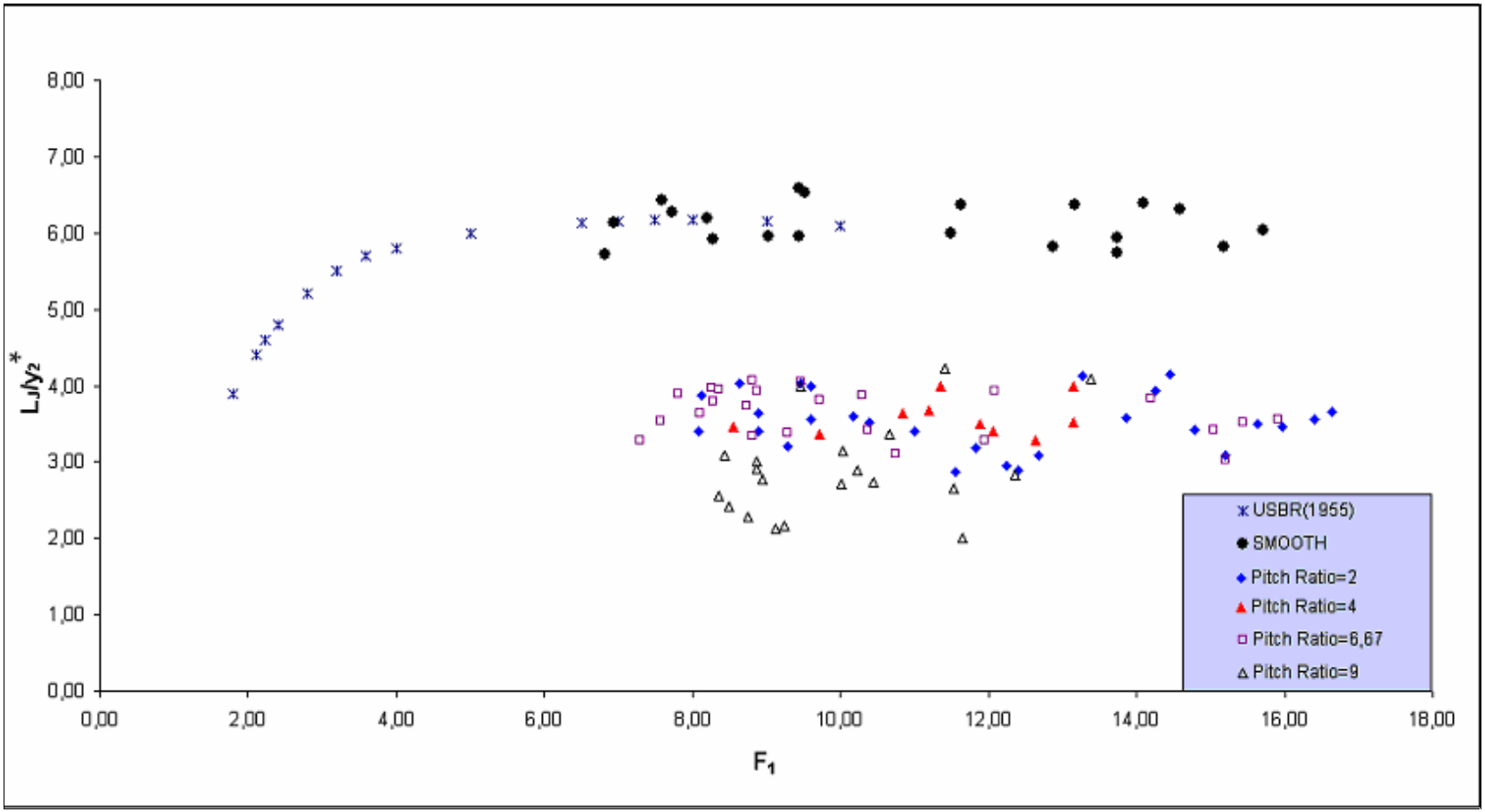

Figure 4.11: Comparison of Relative Jump Length of Rough Beds with That for Smooth Beds

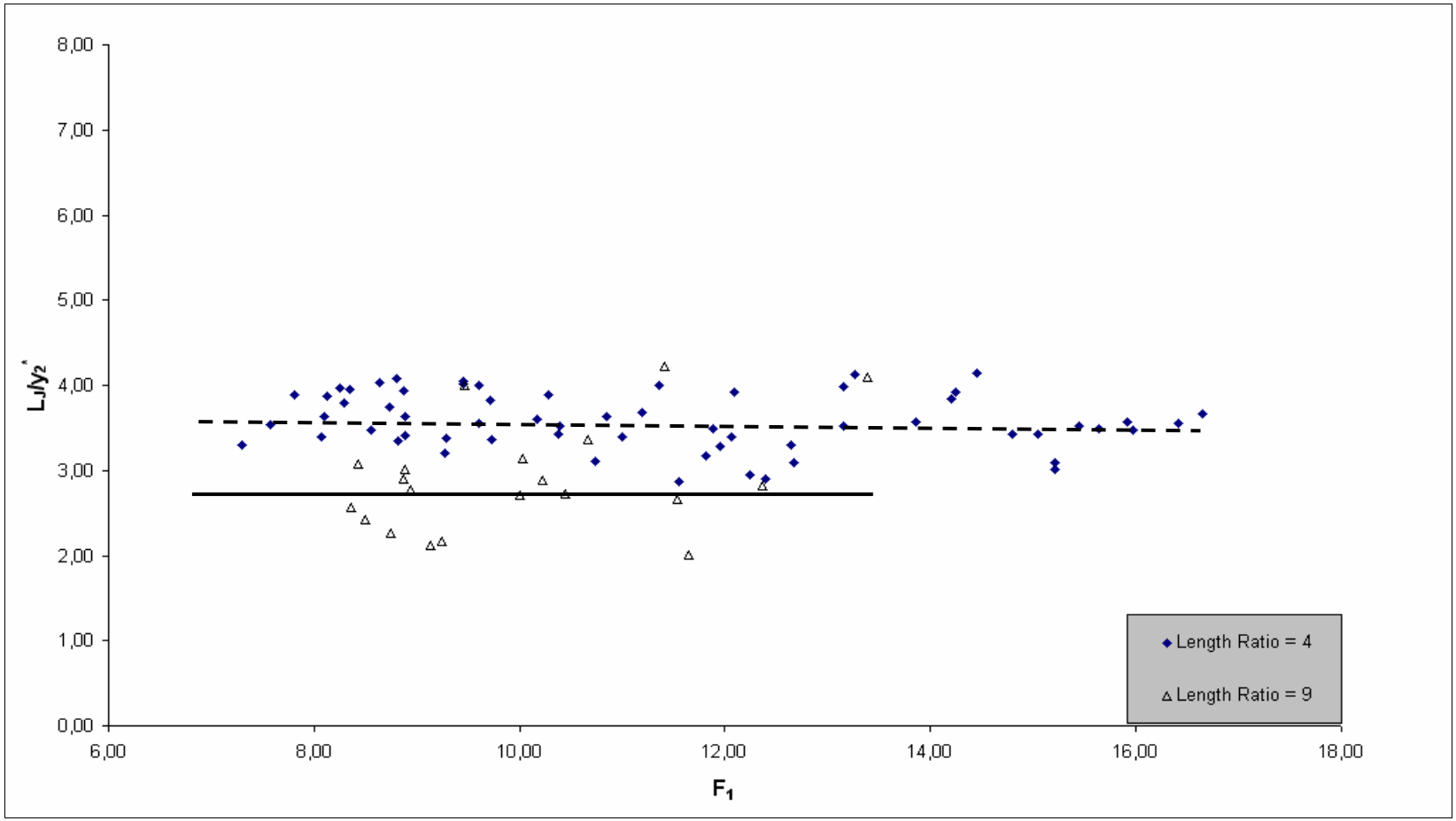

Figure 4.12: Variation of Relative ,jump Length with Froude Number for w / L = 4 and w / L = 9

Fig. 4.11 shows that rough beds decrease the length of hydraulic jump compared with length of the jump on smooth beds. L_j/y_2^* values on smooth beds are in good agreement with *USBR (1955)* data and for smooth beds it is acceptable that, when $F_1>6$, the jump length may be taken as *(USBR, 1955);*

$$L_J = 6.1y_2^* \tag{4.3}$$

Fig 4.12 shows that L_j/y_2^* values for rough beds tend to be constant when the Froude numbers are greater than 6. L_j/y_2^* values are tend to be constant at 3.70 for the length ratio 4 and for the length ratio 9, L_j/y_2^* values tend to be constant at 3.20.

The decrease in the length of the hydraulic jump is about 40%, when the length of hydraulic jumps on smooth beds is compared with that of it on rough beds.

In Fig 4.13, the comparison of effect of different types of roughness on length of the hydraulic jump is shown. L_j/y_2^* versus F_1 values of the experiments with four pitch ratios and experimental data of *Ayanlar(2004) and Ead* and *Rajaratnam (2002)* were used to examine jump properties on corrugated beds. USBR data are also given in Fig. 4.13.

Fig. 4.12 shows that roughness elements and corrugations on channel bed which are not protruding into the flow decrease the length of the jump compared with the jumps on smooth beds. Corrugated beds and rough beds with prismatic roughness elements have practically the same effect on decreasing the length of the hydraulic jump.

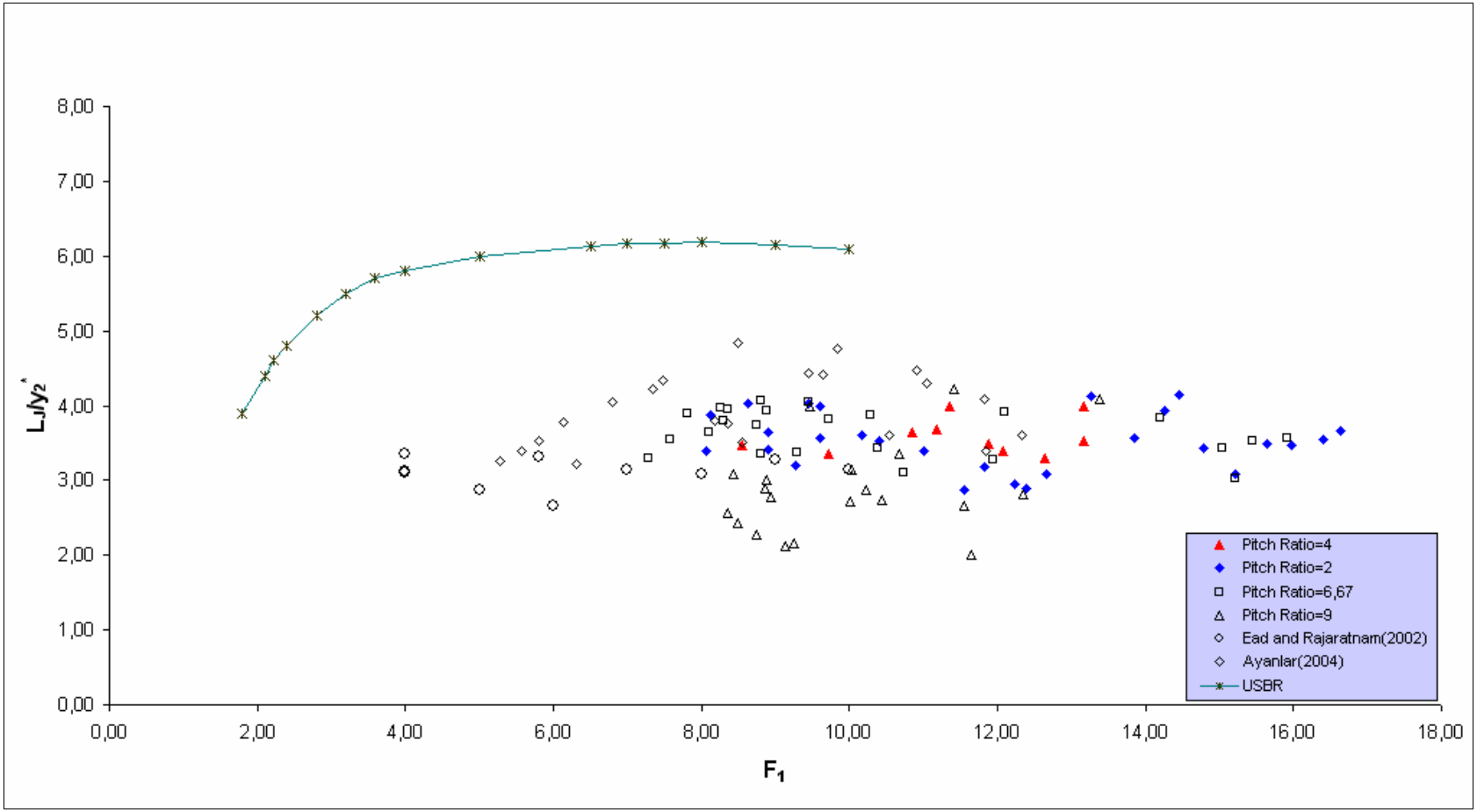

Figure 4.13: Length of Jump for Different Roughness Types

4.6 Gain in Length of Jump

The percent reduction in the length of jump may be expressed as T.

$$T = \frac{L_j^* - L_J}{L_J^*} \times 100 \tag{4.4}$$

where,

T is length reduction ratio

L_j denotes length of jump on rough beds

L_J^* is length of jump that occurs on smooth bed for same incoming Froude number

L_J^* values calculated by the help of Eq. (4.3) and instead of y_2, y_2^* was used in this equation.

Variation of length reduction ratio T with F_1 is shown in Fig 4.14 for different pitch ratios.

Fig 4.14 shows that, an important property of hydraulic jump, length of jump decreases significantly when roughness elements are placed on the channel bed. Length reduction ratio is about 45% for the length ratio 4 and 55% for the length ratio 9 as shown in Fig.4.15.

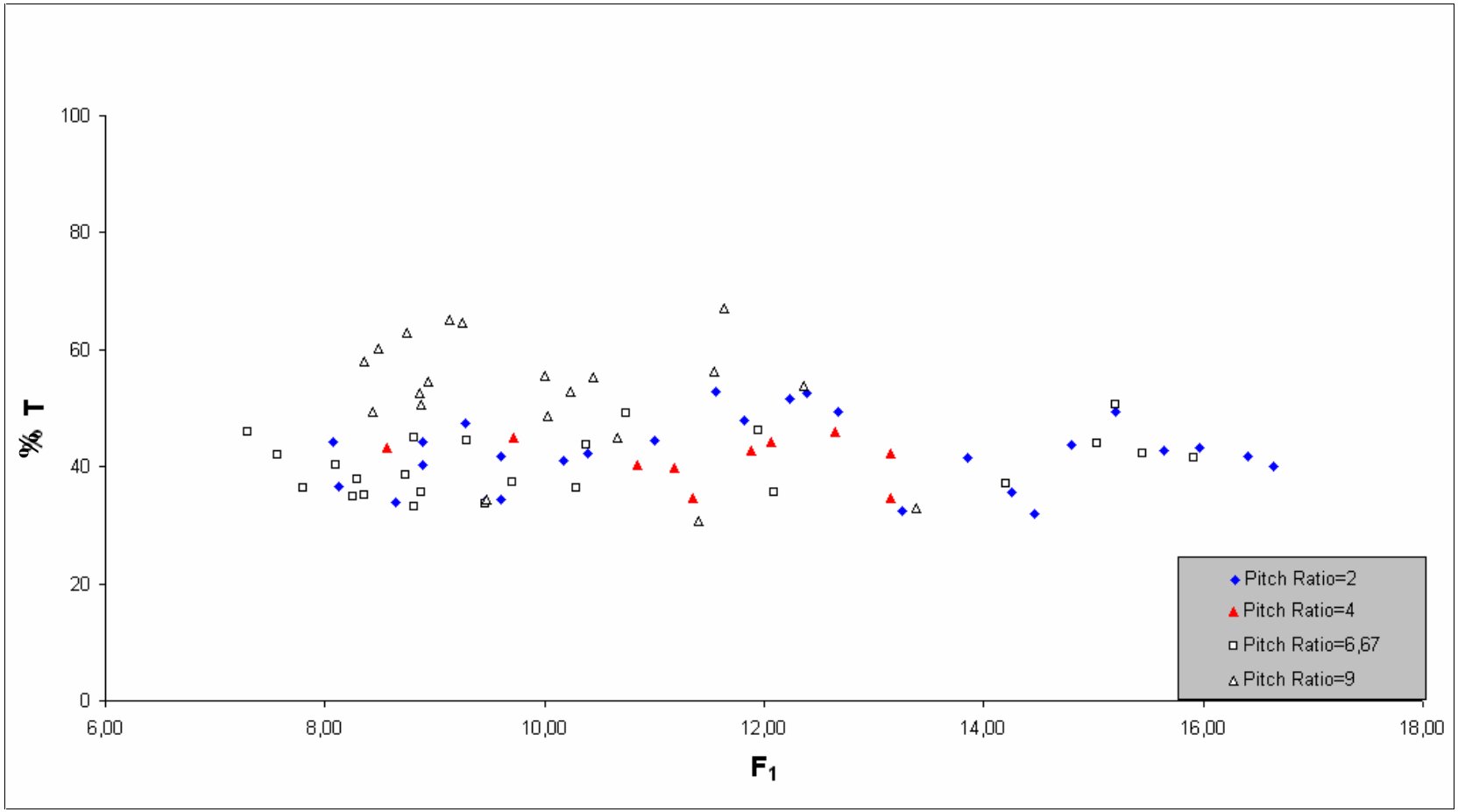

Figure 4.14: Percent Reduction in the Length of Jump for Different Pitch Ratios

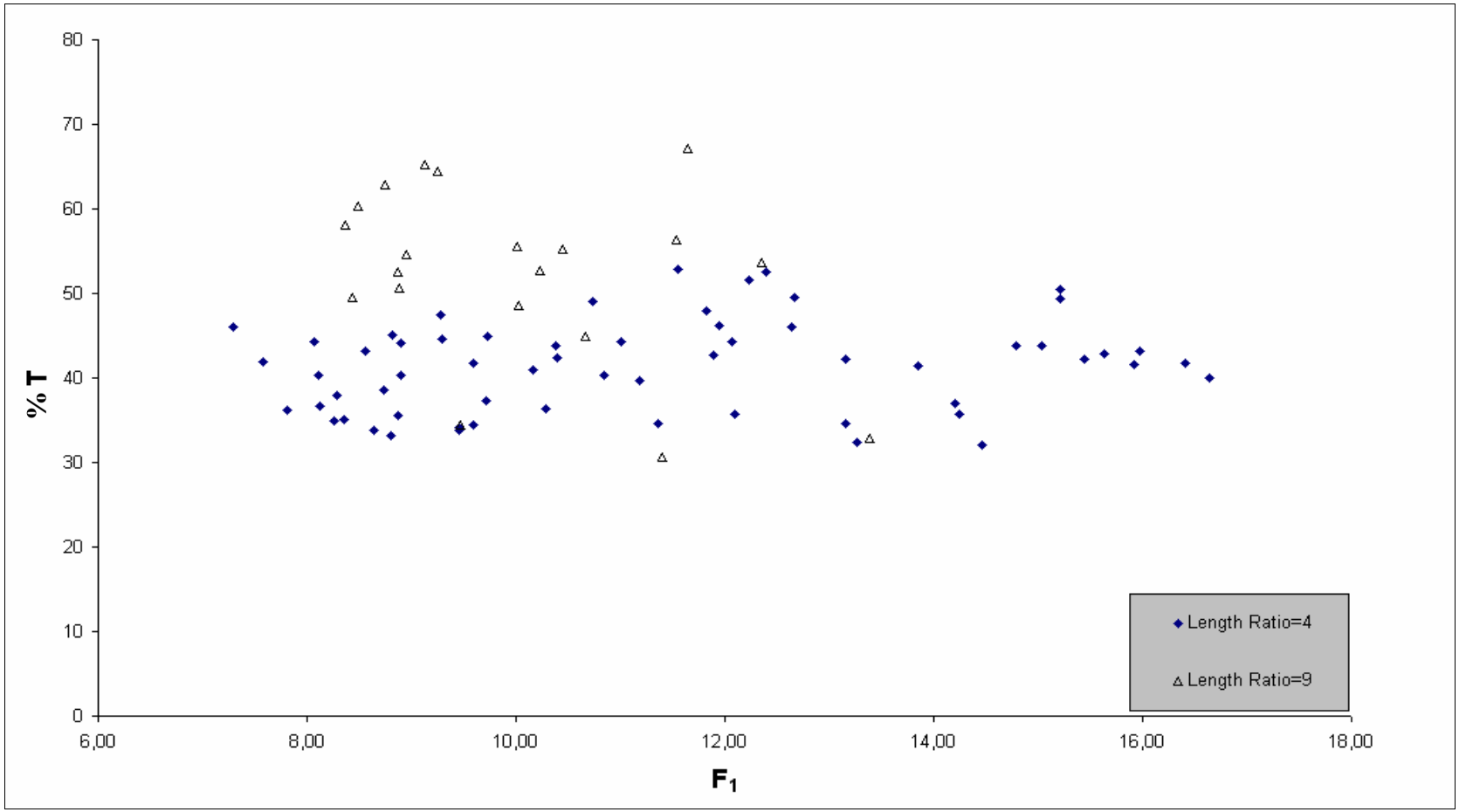

Figure 4.15: Percent Reduction in the Length of Jump for Different Length Ratios

4.7 Energy Loss in the Jump

The specific energy loss E_L, is the difference between the specific energy of incoming flow, E_1 and the specific energy of flow at downstream of the jump, E_2. The relative energy loss, E_L / E_1 is calculated for each set of experiments and the relation between the relative energy loss, E_L / E_1, and incoming Froude number F_1 is shown in Fig. 4.16 for different pitch ratios and smooth channel.

Fig. 4.16 shows that the relative energy loss E_L / E_1 vs. F_1 for different pitch ratios and different length ratios have practically the same effect on energy loss in the hydraulic jumps and energy loss on rough beds slightly higher than experimental results of energy loss values on smooth channel.

To compare different types of roughness, the data of *Ayanlar(2004)* and *Ead and Rajaratnam (2002)* are also shown together with the data of the present study in Fig. 4.17. The wave steepness has the range of $0.19 \leq t/s \leq 0.324$ in data of *Ayanlar(2004)* and *Ead and Rajaratnam (2002)*. Where t is the height of the corrugation and s is the wavelength of the corrugation.

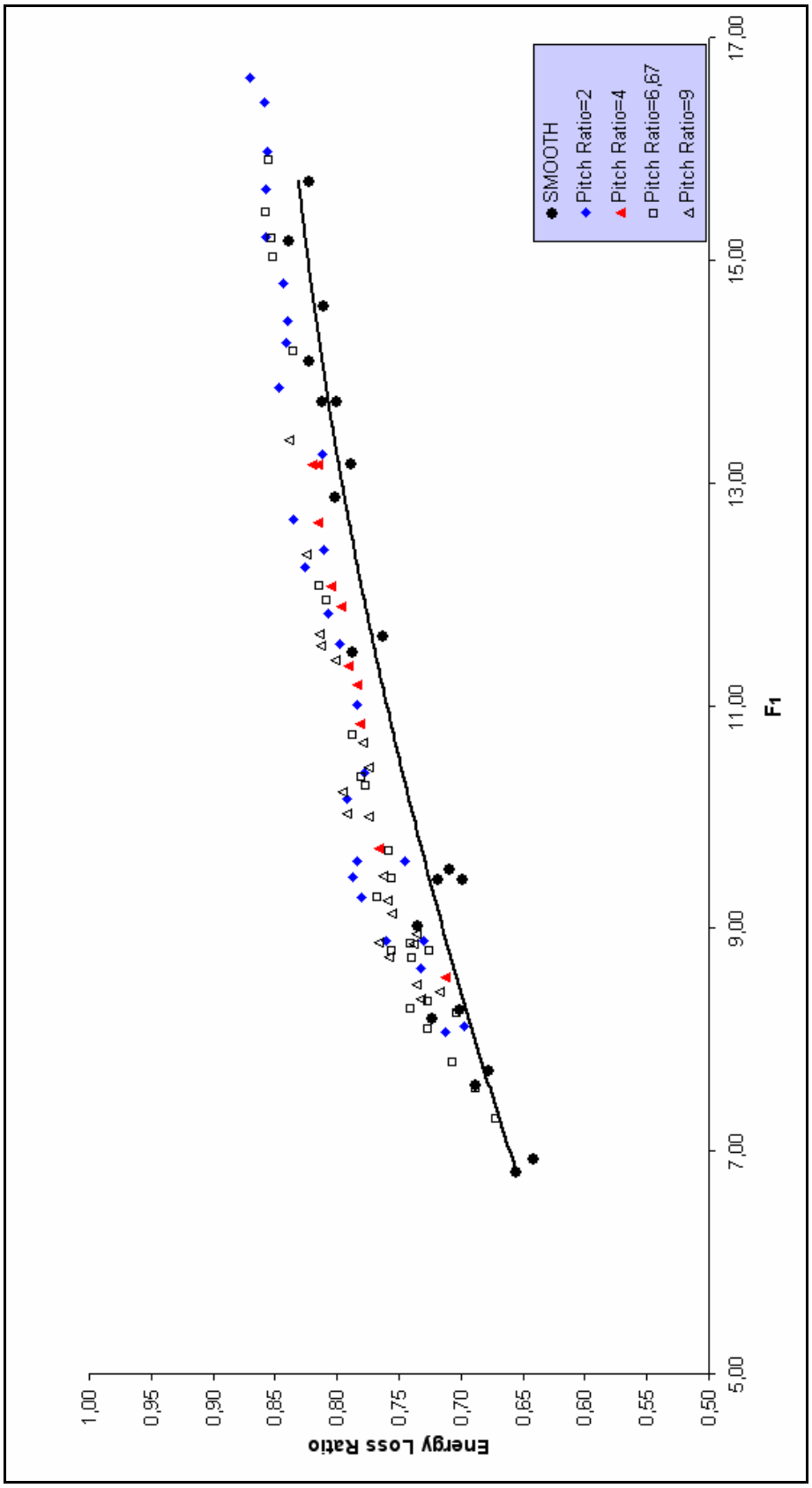

Figure 4. 16: Energy loss Ratio in Jumps for Different Pitch Ratios

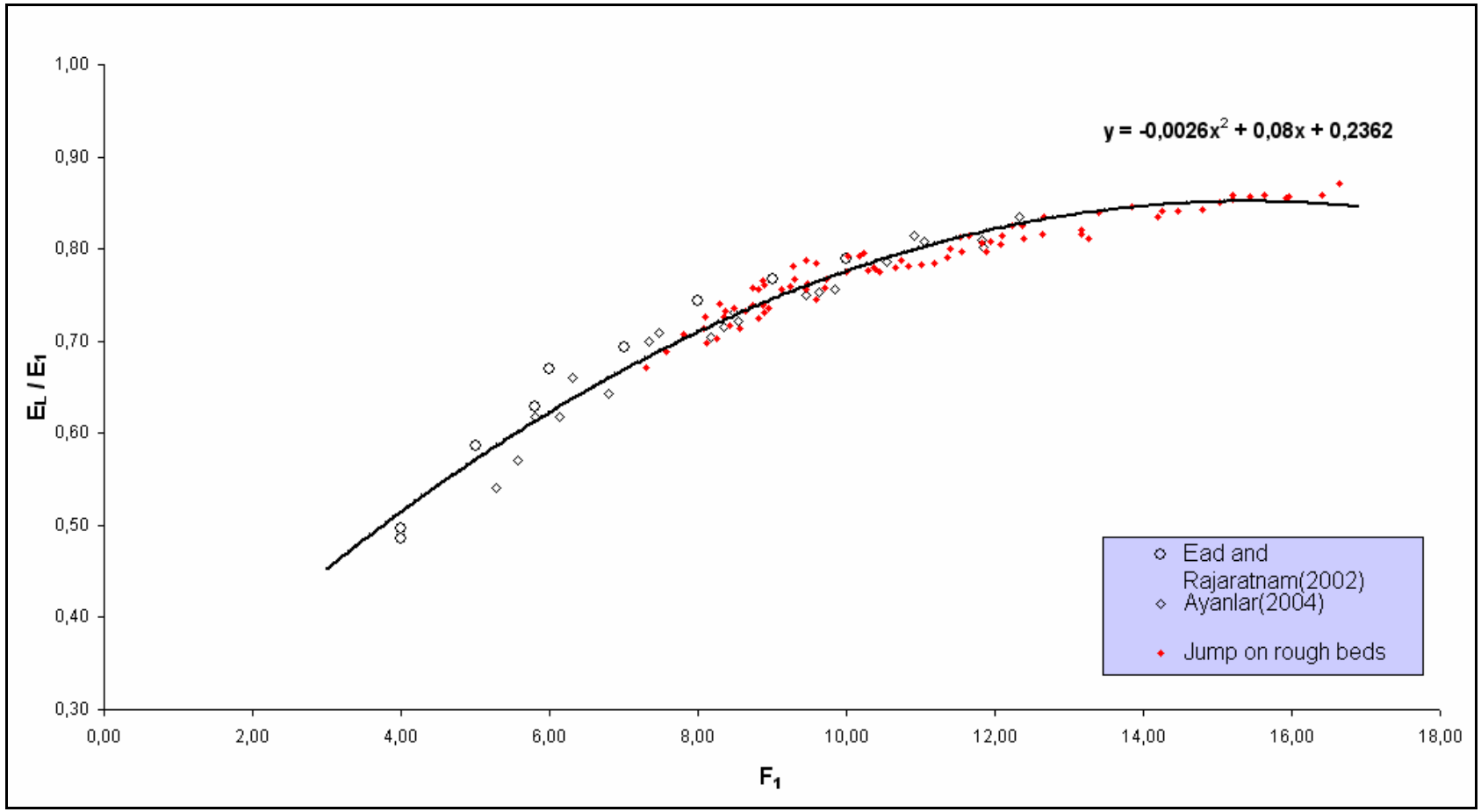

Figure 4. 17: Energy Loss Ratio in Jumps for Different Roughness Types

Fig. 4.17 shows that relative energy loss E_L / E_1 gets closer to 90% of the specific energy of incoming flow asymptotically. It was mentioned in Sec. (2.1.7) that, energy dissipation in the hydraulic jump could be 80% of the specific energy of incoming stream depending on type of the hydraulic jump. It is obvious that ratio of energy dissipation in the hydraulic jump increases with bed roughness. On the other hand, if crests of the roughness or corrugations do not protrude into the flow; vortex structures between two roughness elements or vortex structures between two corrugations do not disturb the flow. The relative energy loss, E_L / E_1 may be expressed as

$$E_L/E_1 = -0{,}0026F_1^2 + 0{,}08F_1 + 0{,}2362 \tag{4.4}$$

4.8 Gain in Energy Dissipation

The percent gain in energy dissipation may be defined as

$$G = \frac{E_L - E_L^*}{E_L} \times 100 \tag{4.5}$$

where,

E_L is the energy loss on a roughened bed

E_L^* is the energy loss of hydraulic jump that occurs on a smooth bed for same incoming Froude number, F_1 and incoming flow depth, y_1.

The variation of the percent gain in energy dissipation G with F_1 is shown in Fig 4.18 for different pitch ratios.

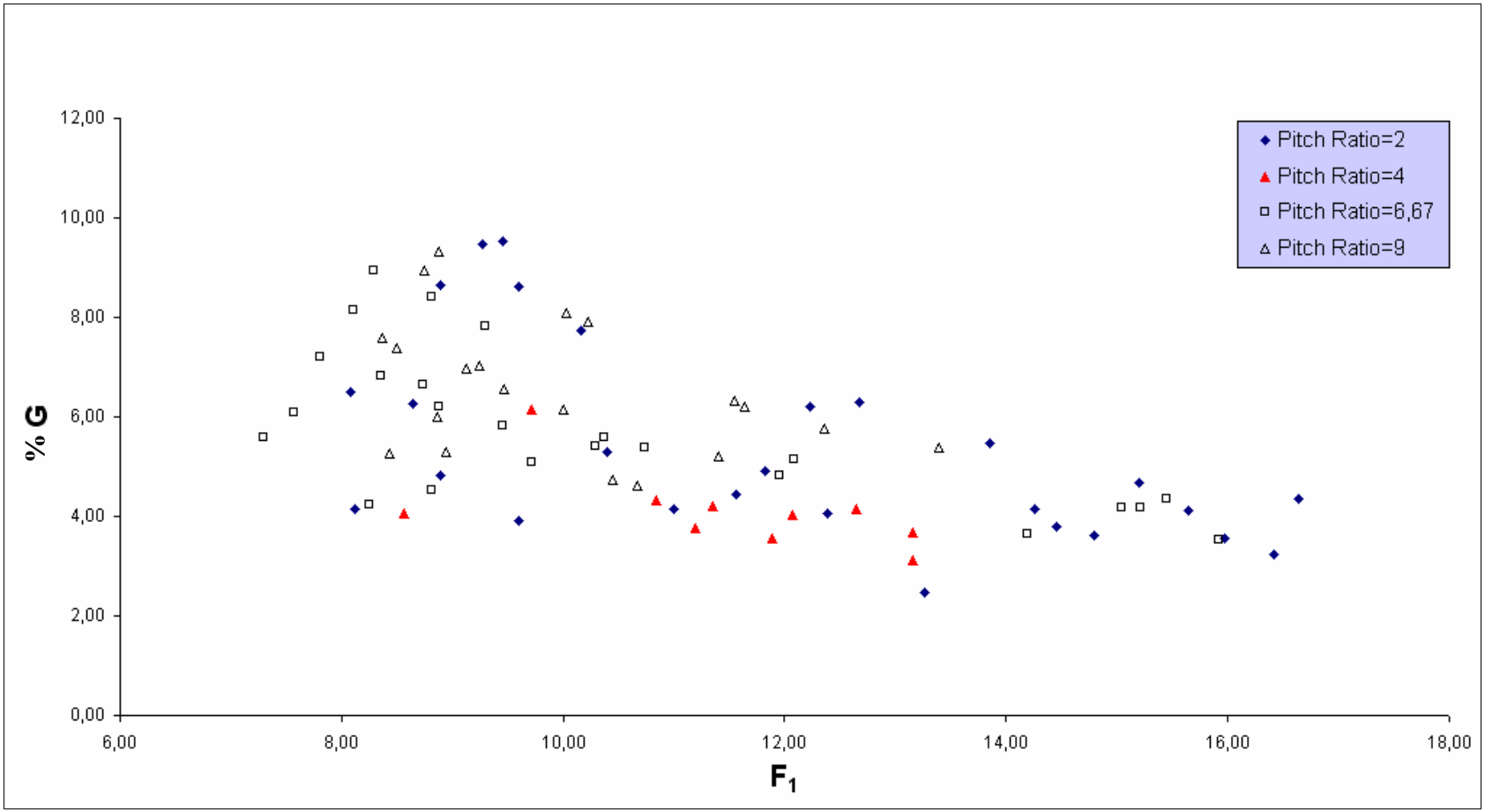

Figure 4. 18: Percent Gain in Energy Dissipation for Different Pitch Ratios

Fig 4.18 shows that the gain in energy loss for the jumps on rough beds decreases as incoming Froude number increases. Gain in energy dissipation does not depend on pitch ratio and length ratio; G values are practically the same at same incoming Froude number F_1 for different pitch and length ratios.

To compare the effect of different roughness types on G, the data compared with data of *Ayanlar(2004)* and *Ead and Rajaratnam (2002)* are shown in Fig. 4.19.

Fig 4.19 shows that if crests of the rib roughness elements and corrugations do not protrude into flow, gain in energy dissipation decreases with increasing incoming Froude number. Furthermore corrugated beds and rough beds have practically the same effect on gain in energy loss with same incoming Froude number.

.

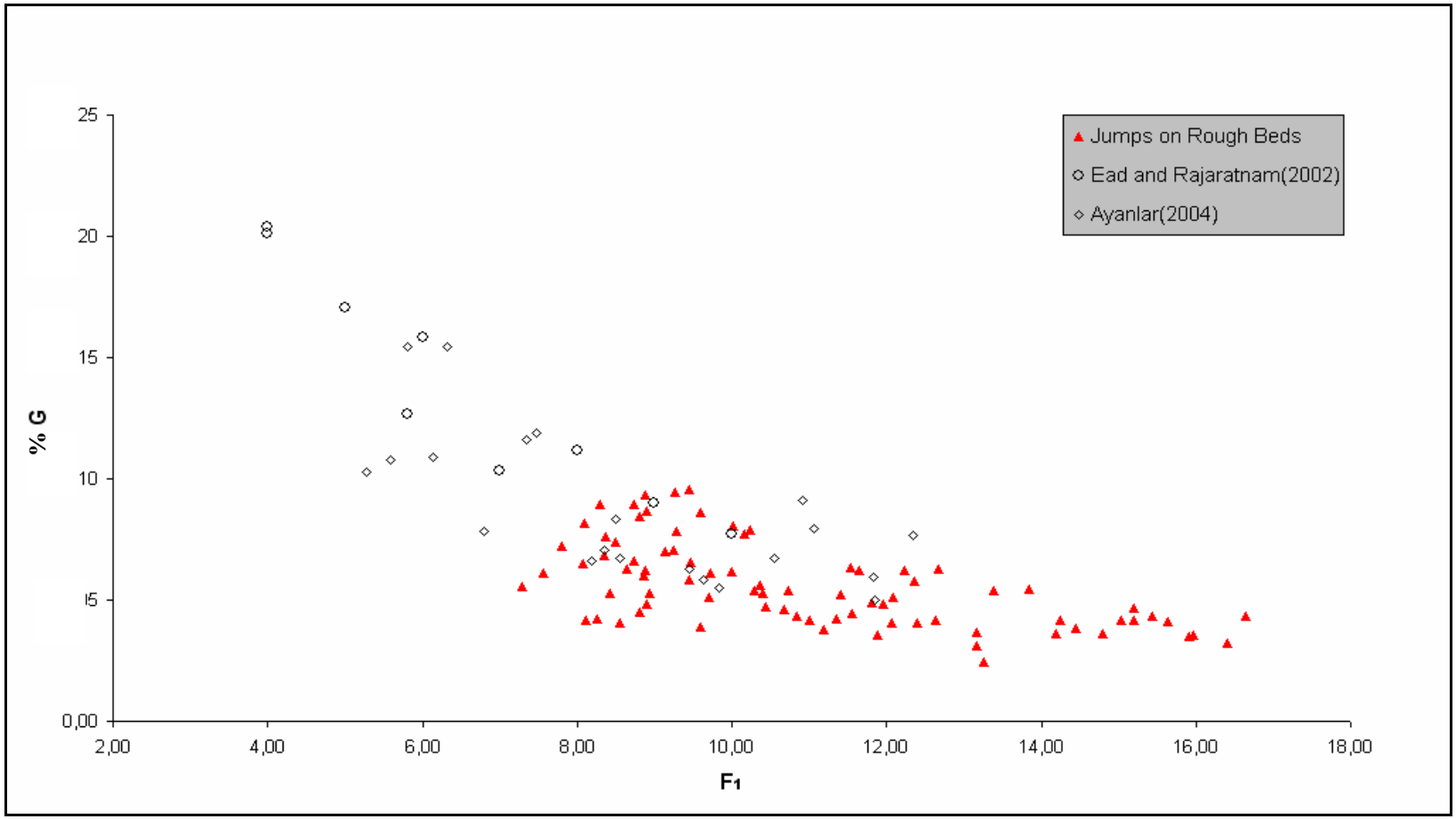

Figure 4. 19: Percent Gain in Energy Dissipation for Different Roughness Types

CHAPTER V

CONCLUSIONS AND RECOMMENDATIONS

The properties of hydraulic jump under a sluice gate in a prismatic, rectangular channel on rough beds are investigated experimentally for a range of Froude numbers 7.3 to 16.6. In the experiments four different pitch ratios and two different length ratios for the roughness elements were used. Hydraulic jump properties on smooth beds were also investigated experimentally. The results of experiments on strip roughness placed perpendicular to the flow direction with different pitch ratios were compared with the results of experiments performed on smooth beds and corrugated beds data available in literature.

From this study the following conclusions are reached:

1. For a given upstream condition y_1 and F_1, the tailwater depth to form the jump on a rough bed is about 20% smaller than the jump on a smooth bed, for Froude number range of $7{,}30 \leq F_1 \leq 16{,}60$, and the length ratio range of $4 \leq w/L \leq 9$.

2. The length of jump is taken as the distance between toe of jump and the section where $y = 0.99\ y_2$. This length on rough beds is about 40% shorter than that for on smooth beds.

3. The energy loss in hydraulic jump on rough beds is 5 – 10 % larger than that for free jump on smooth beds.

4. Vortexes formed between two successive roughness elements increase shear stresses. Increase in energy loss, reduction in required tail water depth and length of the jump are physical outcomes of increased shear stress.

5. Jump parameters such as depth ratio, reduction in tail water depth, length of jump, energy loss along jump and gain in energy dissipation in hydraulic jump on rough beds are practically the same with corrugated beds when geometric properties of corrugations are similar to the roughened beds with strip roughness.

6. These results show that strip roughness placed perpendicular to the flow may be a good alternative to baffle blocks and sills in stilling basins where flow velocity is high.

The study can be expanded by investigating the effects of different pitch and length ratios on the jump properties. To overcome dominancy of the first roughness element, hydraulic jump can be forced to start at the first roughness element for the same experimental setup, so the effect of higher pitch ratios on the energy dissipation, the depth ratio and the length of the jump should be further investigated.

REFERENCES

ALHAMID, A.A., and NEGM, A.A., (1996), Depth Ratio of Hydraulic Jump in Rectangular Stilling Basins, Journal of Hydraulic Engineering, Vol.34, No.4, pp.597-604.

AYANLAR, KÜRŞAD (2004), Hydraulic Jump On Corrugated Beds, Ms. Thesis, Middle East Technical University, Department of Civil Engineering, Ankara, Turkey.

BAKHMETEFF, B.A. and MATZKE, A. E. (1936), The Hydraulic Jump in Terms of Dynamic Similarity, Trans. ASCE Vol. 101 pp. 630-680., (ed), RAJARATNAM, N., and SUBRAMANYA, K., (1968), Profiles of the Hydraulic Jump, Journal of Hydraulic Division, Vol.94, No.3, pp. 663-673.

BRETZ, N. V. (1987), Ressaut Hydraulique Forcé par Seuil (Hydraulic Jump Forced By Sills), Thèse no. 669 présentée au Département de Génie Civil, Ecole Polytechnique Fédérale de Lausanne, pour I'obtention du Grade de Docteur ès Sciences Techniques, Lausanne., (ed), HAGER, W. H., and BREMEN, R.(1989), Classical Hydraulic Jump: Sequent Depths, Journal of Hydraulic Research, Vol.27(5), pp. 565-585.

CHOW, V.T., (1959), Open-Channel Hydraulics, McGraw-Hill, New York.

JIE CUI, V.C. PATEL and CHING-LONG LIN,(2003) Large-eddy Simulation of Turbulent flow in a Channel with Rib Roughness, International Journal of Heat and Fluid Flow, 24 (2003), pp. 372-388

ÇELİK, H.Ç., BİROL, B., GOĞÜŞ, M., Effect of Roughness on Hydraulic Jump Properties, I. National Hydraulic Engineering Symposium / IZMIR, 22-26 September 2003.

EAD, S.A., and RAJARATNAM, N., (2002), Hydraulic Jump on Corrugated Beds, Journal of Hydraulic Engineering, Vol.128, No.7, pp. 656-662.

EAD, S.A., RAJARATNAM, N., KATOPODIS, C., and ADE, F., (2000), Turbulent Open-Channel Flow in Circular Corrugated Culverts, Journal of Hydraulic Engineering, Vol.126, No.10, pp. 750-757.

ELEVATORSKI, E.A., (1959), Hydraulic Energy Dissipaters, McGraw-Hill, New York.

HAGER, W. H., and BREMEN, R.(1989), Classical Hydraulic Jump: Sequent Depths, Journal of Hydraulic Research, Vol.27(5), pp. 565-585.

HARLEMAN, D. R. F.(1959), Discussion to Rouse, et al. (1959), Trans. ASCE, Vol. 124, pp. 959-962. (ed), HAGER, W. H., and BREMEN, R.(1989), Classical Hydraulic Jump: Sequent Depths, Journal of Hydraulic Research, Vol.27(5), pp. 565-585.

HUGHES, W.C., and FLACK, J.E., (1984), Hydraulic Jump Properties Over a Rough Bed, Journal of Hydraulic Engineering, Vol. 110, No.12, pp. 1755-1771.

LEUTHEUSSER, H.J. and KARTHA, V.J. (1972), Effects of Inflow Condition on Hydraulic Jump, Proc. ASCE J. Hydraulic Division, Vol. 98, HY8, pp 1367-1385., (ed), HAGER, W. H., and BREMEN, R.(1989), Classical Hydraulic Jump: Sequent Depths, Journal of Hydraulic Research, Vol.27(5), pp. 565-585.

MOHAMED ALI, H.S., (1991), Effect of Roughened Bed Stilling Basin on Length of Rectangular Hydraulic Jump, Journal of Hydraulic Engineering, Vol.117, No.1, pp. 83-93.

NEGM, A.A.M., (2002), Optimal Roughened Length of Prismatic Stilling Basins, ICHE 2002 / Warshaw, 2002.

OHTSU, I. and YASUDA Y.(1994), Characteristics of Supercritical Flow Below a Sluice Gate, Journal of Hydraulic Engineering, 1994, 120(3), pp. 332-345

PERRY, A. E., SCHOFIELD, W.H. and JOUBERT, P. N. (1969), Rough-wall Turbulent Boundary Layers, Journal of Fluid Mech., Vol. 37, pp. 383-413,

PETERKA, A.J., (1958), Hydraulic Designs of Stilling Basins and Energy Dissipators, Engineering Monograph, No.25, U.S. Bureau of Reclamation, Denver.

RAJARATNAM N. (1965), The Hydraulic Jump as a Wall Jet, Journal of Hydraulics Division 1965, 91(5) pp. 107-132

RAJARATNAM, N., and SUBRAMANYA, K., (1968), Profiles of the Hydraulic Jump, Journal of Hydraulic Division, Vol.94, No.3, pp. 663-673.

TANI I.(1987), Turbulent Boundary Layer Development over Rough Surface, Perspective in Turbulence Studies, Editor; Meier H.U. and Bradshaw P., Springer-Verlag, pp.223-249.

U.S.B.R., (1955), Research Studies on Stilling Basins, Energy Dissipators and Associated Appurtenances, U.S. Bureau of Reclamation, Hydraulic Laboratory Report No. Hyd-399.

APPENDIX A

EXPERIMENTAL MEASUREMENTS AND CALCULATIONS

TABLE A.1: Tabular Form of Experiments on Rough Beds

SET	Z (cm)	W (cm)	H (cm)	Q (l/s)	y_1 (cm)	y_2 (cm)	F_1	F_2	J_{start} (cm)	J_{end} (cm)	L_j (cm)
1	1	4	24.15	10.52	1.11	14.75	11.35	0.23	157	226	69
2	1	4	24.06	10.42	1.07	15.20	11.89	0.22	93	154	61
3	1	4	25.20	11.70	1.08	17.08	13.16	0.21	127	196	69
4	1	4	25.20	11.70	1.08	16.60	13.16	0.22	78	156	78
5	1	4	26.76	13.60	1.33	17.79	11.19	0.23	78	153	75
6	1	4	27.83	15.00	1.35	19.00	12.07	0.23	102	178	76
7	1	4	28.73	16.24	1.38	20.06	12.64	0.23	145	224	79
8	1	4	25.75	12.35	1.37	14.87	9.72	0.27	106	167	61
9	1	4	24.15	10.52	1.34	14.02	8.56	0.25	63	117	54
10	1	4	26.90	13.78	1.37	17.43	10.84	0.24	130	204	74
11	1	9	24.29	10.68	1.36	12.74	8.49	0.30	56	94	38
12	1	9	25.80	12.41	1.46	13.08	8.88	0.33	90	143	53
13	1	9	27.08	14.01	1.54	15.56	9.25	0.29	123	165	42
14	1	9	27.08	14.01	1.44	14.98	10.23	0.30	82	140	58
15	1	9	25.84	12.46	1.35	13.76	10.03	0.31	48	106	58
16	1	9	24.46	10.86	1.28	13.39	9.47	0.28	-5	61	66
17	1	9	24.52	10.93	1.02	14.44	13.39	0.25	0	77	77

SET	Z (cm)	W (cm)	H (cm)	Q (l/s)	y_1 (cm)	y_2 (cm)	F_1	F_2	J_{start} (cm)	J_{end} (cm)	L_j (cm)
18	1	9	25.6	12.17	1.21	14.73	11.54	0.27	86	137	51
19	1	9	26.57	13.36	1.23	16.14	12.36	0.26	121	180	59
20	1	9	26.57	13.36	1.28	15.76	11.64	0.27	164	205	41
21	1	9	25.48	12.03	1.21	15.43	11.41	0.25	127	207	80
22	1	9	24.23	10.61	1.18	14.32	10.45	0.25	84	130	46
23	1	9	27.85	15.03	1.66	16.86	8.87	0.27	0	58	58
24	1	9	28.85	16.41	1.75	18.32	8.95	0.26	25	84	59
25	1	9	29.78	17.77	1.82	18.25	9.13	0.29	80	128	48
26	1	9	29.78	17.77	1.93	17.75	8.36	0.30	98	154	56
27	1	9	28.88	16.46	1.78	16.05	8.74	0.32	58	106	48
28	1	9	27.98	15.20	1.73	17.24	8.43	0.27	21	82	61
29	1	9	29.88	17.92	1.65	20.47	10.67	0.24	-5	76	81
30	1	9	30.79	19.31	1.81	20.08	10.01	0.27	67	134	67
31	2	4	26.10	12.78	1.36	14.22	10.17	0.30	96	164	68
32	2	4	26.10	12.78	1.34	15.84	10.39	0.26	68	135	67
33	2	4	26.10	12.78	1.29	16.74	11.01	0.24	3	69	66
34	2	4	27.23	14.21	1.29	16.42	12.24	0.27	32	96	64
35	2	4	27.23	14.21	1.32	17.54	11.82	0.24	106	174	68
36	2	4	27.23	14.21	1.34	17.88	11.56	0.24	157	218	61
37	2	4	28.25	15.57	1.36	19.54	12.39	0.23	189	256	67
38	2	4	28.25	15.57	1.34	17.34	12.67	0.27	146	218	72
39	2	4	28.25	15.57	1.30	21.34	13.26	0.20	69	167	98
40	2	4	25.58	12.15	1.07	15.42	13.85	0.25	143	216	73
41	2	4	25.58	12.15	1.05	16.75	14.25	0.22	87	168	81
42	2	4	25.58	12.15	1.04	17.11	14.46	0.22	53	139	86
43	2	4	26.70	13.52	1.06	18.12	15.64	0.22	57	137	80
44	2	4	26.70	13.52	1.08	17.45	15.21	0.23	138	208	70
45	2	4	26.70	13.52	1.10	18.65	14.79	0.21	187	264	77
46	2	4	27.68	14.80	1.11	20.04	15.97	0.21	236	321	85
47	2	4	27.68	14.80	1.09	20.52	16.41	0.20	187	275	88
48	2	4	27.68	14.80	1.08	18.98	16.64	0.23	103	194	91
49	2	4	27.69	14.81	1.75	16.21	8.07	0.29	117	182	65

SET	Z (cm)	W (cm)	H (cm)	Q (l/s)	y_1 (cm)	y_2 (cm)	F_1	F_2	J_{start} (cm)	J_{end} (cm)	L_j (cm)
18	1	9	25.6	12.17	1.21	14.73	11.54	0.27	86	137	51
19	1	9	26.57	13.36	1.23	16.14	12.36	0.26	121	180	59
20	1	9	26.57	13.36	1.28	15.76	11.64	0.27	164	205	41
21	1	9	25.48	12.03	1.21	15.43	11.41	0.25	127	207	80
22	1	9	24.23	10.61	1.18	14.32	10.45	0.25	84	130	46
23	1	9	27.85	15.03	1.66	16.86	8.87	0.27	0	58	58
24	1	9	28.85	16.41	1.75	18.32	8.95	0.26	25	84	59
25	1	9	29.78	17.77	1.82	18.25	9.13	0.29	80	128	48
26	1	9	29.78	17.77	1.93	17.75	8.36	0.30	98	154	56
27	1	9	28.88	16.46	1.78	16.05	8.74	0.32	58	106	48
28	1	9	27.98	15.20	1.73	17.24	8.43	0.27	21	82	61
29	1	9	29.88	17.92	1.65	20.47	10.67	0.24	-5	76	81
30	1	9	30.79	19.31	1.81	20.08	10.01	0.27	67	134	67
31	2	4	26.10	12.78	1.36	14.22	10.17	0.30	96	164	68
32	2	4	26.10	12.78	1.34	15.84	10.39	0.26	68	135	67
33	2	4	26.10	12.78	1.29	16.74	11.01	0.24	3	69	66
34	2	4	27.23	14.21	1.29	16.42	12.24	0.27	32	96	64
35	2	4	27.23	14.21	1.32	17.54	11.82	0.24	106	174	68
36	2	4	27.23	14.21	1.34	17.88	11.56	0.24	157	218	61
37	2	4	28.25	15.57	1.36	19.54	12.39	0.23	189	256	67
38	2	4	28.25	15.57	1.34	17.34	12.67	0.27	146	218	72
39	2	4	28.25	15.57	1.30	21.34	13.26	0.20	69	167	98
40	2	4	25.58	12.15	1.07	15.42	13.85	0.25	143	216	73
41	2	4	25.58	12.15	1.05	16.75	14.25	0.22	87	168	81
42	2	4	25.58	12.15	1.04	17.11	14.46	0.22	53	139	86
43	2	4	26.70	13.52	1.06	18.12	15.64	0.22	57	137	80
44	2	4	26.70	13.52	1.08	17.45	15.21	0.23	138	208	70
45	2	4	26.70	13.52	1.10	18.65	14.79	0.21	187	264	77
46	2	4	27.68	14.80	1.11	20.04	15.97	0.21	236	321	85
47	2	4	27.68	14.80	1.09	20.52	16.41	0.20	187	275	88
48	2	4	27.68	14.80	1.08	18.98	16.64	0.23	103	194	91
49	2	4	27.69	14.81	1.75	16.21	8.07	0.29	117	182	65

SET	Z (cm)	W (cm)	H (cm)	Q (l/s)	y_1 (cm)	y_2 (cm)	F_1	F_2	J_{start} (cm)	J_{end} (cm)	L_j (cm)
50	2	4	27.66	14.77	1.74	17.32	8.12	0.26	98	172	74
51	2	4	27.66	14.77	1.67	16.46	8.64	0.28	5	84	79
52	2	4	28.78	16.31	1.68	15.44	9.45	0.34	21	108	87
53	2	4	28.78	16.31	1.75	16.14	8.89	0.32	107	184	77
54	2	4	28.78	16.31	1.75	18.5	8.89	0.26	156	228	72
55	2	4	29.57	17.46	1.78	16.25	9.28	0.34	190	262	72
56	2	4	29.57	17.46	1.74	20.25	9.60	0.24	127	208	81
57	2	4	29.57	17.46	1.74	16.84	9.60	0.32	68	159	91
58	0.6	4	27.10	14.04	1.30	17.48	11.95	0.24	56	126	70
59	0.6	4	27.10	14.04	1.29	17.24	12.09	0.25	12	96	84
60	0.6	4	28.90	16.48	1.29	21.13	14.20	0.21	12	109	97
61	0.6	4	30.39	18.69	1.30	23.46	15.91	0.21	11	113	102
62	0.6	4	30.39	18.69	1.34	22.37	15.21	0.22	96	181	85
63	0.6	4	30.39	18.69	1.35	22.38	15.04	0.22	72	168	96
64	0.6	4	29.89	17.93	1.29	21.54	15.45	0.23	16	113	97
65	0.6	4	30.61	19.03	1.76	20.54	10.29	0.26	81	177	96
66	0.6	4	30.61	19.03	1.71	20.67	10.74	0.26	29	107	78
67	0.6	4	30.61	19.03	1.75	20.41	10.37	0.26	63	148	85
68	0.6	4	29.09	16.76	1.71	18.38	9.46	0.27	17	106	89
69	0.6	4	29.09	16.76	1.68	18.96	9.71	0.26	32	117	85
70	0.6	4	29.09	16.76	1.73	16.99	9.29	0.30	72	146	74
71	0.6	4	28.38	15.75	1.72	18.22	8.81	0.26	48	117	69
72	0.6	4	27.55	14.63	1.71	17.23	8.25	0.26	22	98	76
73	0.6	4	29.15	16.84	2.04	17.79	7.29	0.28	62	128	66
74	0.6	4	29.15	16.84	1.99	17.69	7.57	0.29	26	98	72
75	0.6	4	29.15	16.84	1.95	17.22	7.81	0.30	13	93	80
76	0.6	4	30.78	19.30	1.98	19.45	8.74	0.28	56	144	88
77	0.6	4	30.78	19.30	1.96	19.78	8.87	0.28	24	117	93
78	0.6	4	30.78	19.30	1.97	18.22	8.81	0.31	12	108	96
79	0.6	4	29.86	17.89	1.98	17.45	8.10	0.31	58	137	79
80	0.6	4	29.86	17.89	1.95	16.98	8.29	0.32	19	102	83
81	0.6	4	29.86	17.89	1.94	18.28	8.35	0.29	9	96	87

TABLE A.2: Tabular Form of Experiments on Smooth Beds

SET	Z (cm)	W (cm)	H (cm)	Q (l/s)	y_1 (cm)	y_2 (cm)	F_1	F_2	J_{start} (cm)	J_{end} (cm)	L_j (cm)
1	-	-	27.92	15.12	1.30	21.22	12.87	0.20	120	254	134
2	-	-	27.92	15.12	1.28	23.38	13.18	0.17	24	172	148
3	-	-	28.65	16.13	1.30	22.98	13.73	0.18	112	253	141
4	-	-	28.65	16.13	1.30	24.43	13.73	0.17	43	189	146
5	-	-	29.22	16.94	1.29	25.95	14.59	0.16	54	218	164
6	-	-	29.22	16.94	1.32	23.18	14.10	0.19	157	321	164
7	-	-	30.10	18.25	1.32	24.32	15.19	0.19	93	254	161
8	-	-	30.10	18.25	1.29	28.21	15.72	0.15	127	296	169
9	-	-	26.68	13.50	1.29	20.67	11.63	0.18	78	209	131
10	-	-	26.68	13.50	1.30	18.12	11.49	0.22	78	201	123
11	-	-	25.43	11.97	1.68	14.58	6.94	0.27	102	198	96
12	-	-	25.43	11.97	1.70	13.56	6.82	0.30	145	234	89
13	-	-	26.56	13.35	1.70	15.22	7.60	0.28	106	218	112
14	-	-	26.56	13.35	1.68	16.23	7.74	0.26	63	173	110
15	-	-	27.38	14.40	1.69	17.21	8.27	0.25	130	242	112
16	-	-	27.38	14.40	1.70	15.65	8.20	0.29	56	173	117
17	-	-	28.66	16.14	1.72	18.43	9.03	0.26	90	216	126
18	-	-	28.66	16.14	1.67	22.48	9.44	0.19	123	251	128
19	-	-	29.08	16.74	1.70	22.54	9.53	0.20	82	226	144
20	-	-	29.08	16.74	1.71	21.45	9.45	0.21	48	193	145

APPENDIX B

EXPERIMENTAL DATA OF PAST WORKS

B.1: Experimental Data of AYANLAR (2004)

TABLE B.1: Tabular Form of Data for t = 10 mm *(AYANLAR, 2004)*

Set	y_1 (cm)	Q (m^3/sec)	F_1	y_2 (cm)	L_J (cm)	x_J (cm)
5	1.1650	0.009418	9.451425	13.1959	70	55
6	1.1500	0.009418	9.6369458	13.4061	70	20
7	1.1750	0.011157	11.054098	13.7984	80	95
8	1.2700	0.011157	9.8372687	15.2167	85	65
9	1.5500	0.011426	7.4721587	12.7151	72	55
10	1.6500	0.011426	6.8032702	14.0203	65	25
22	1.0500	0.007286	8.5458355	10.8899	45	20
23	0.9200	0.00572	8.1803823	9.2651	41	15
44	1.3600	0.010672	8.4911751	13.3924	80	0
45	1.3000	0.013892	11.827947	17.4535	90	5

TABLE A.2: Tabular Form of Experiments on Smooth Beds

SET	Z (cm)	W (cm)	H (cm)	Q (l/s)	y_1 (cm)	y_2 (cm)	F_1	F_2	J_{start} (cm)	J_{end} (cm)	L_j (cm)
1	-	-	27.92	15.12	1.30	21.22	12.87	0.20	120	254	134
2	-	-	27.92	15.12	1.28	23.38	13.18	0.17	24	172	148
3	-	-	28.65	16.13	1.30	22.98	13.73	0.18	112	253	141
4	-	-	28.65	16.13	1.30	24.43	13.73	0.17	43	189	146
5	-	-	29.22	16.94	1.29	25.95	14.59	0.16	54	218	164
6	-	-	29.22	16.94	1.32	23.18	14.10	0.19	157	321	164
7	-	-	30.10	18.25	1.32	24.32	15.19	0.19	93	254	161
8	-	-	30.10	18.25	1.29	28.21	15.72	0.15	127	296	169
9	-	-	26.68	13.50	1.29	20.67	11.63	0.18	78	209	131
10	-	-	26.68	13.50	1.30	18.12	11.49	0.22	78	201	123
11	-	-	25.43	11.97	1.68	14.58	6.94	0.27	102	198	96
12	-	-	25.43	11.97	1.70	13.56	6.82	0.30	145	234	89
13	-	-	26.56	13.35	1.70	15.22	7.60	0.28	106	218	112
14	-	-	26.56	13.35	1.68	16.23	7.74	0.26	63	173	110
15	-	-	27.38	14.40	1.69	17.21	8.27	0.25	130	242	112
16	-	-	27.38	14.40	1.70	15.65	8.20	0.29	56	173	117
17	-	-	28.66	16.14	1.72	18.43	9.03	0.26	90	216	126
18	-	-	28.66	16.14	1.67	22.48	9.44	0.19	123	251	128
19	-	-	29.08	16.74	1.70	22.54	9.53	0.20	82	226	144
20	-	-	29.08	16.74	1.71	21.45	9.45	0.21	48	193	145

APPENDIX B

EXPERIMENTAL DATA OF PAST WORKS

B.1: Experimental Data of AYANLAR (2004)

TABLE B.1: Tabular Form of Data for t = 10 mm *(AYANLAR, 2004)*

Set	y_1 (cm)	Q (m^3/sec)	F_1	y_2 (cm)	L_J (cm)	x_J (cm)
5	1.1650	0.009418	9.451425	13.1959	70	55
6	1.1500	0.009418	9.6369458	13.4061	70	20
7	1.1750	0.011157	11.054098	13.7984	80	95
8	1.2700	0.011157	9.8372687	15.2167	85	65
9	1.5500	0.011426	7.4721587	12.7151	72	55
10	1.6500	0.011426	6.8032702	14.0203	65	25
22	1.0500	0.007286	8.5458355	10.8899	45	20
23	0.9200	0.00572	8.1803823	9.2651	41	15
44	1.3600	0.010672	8.4911751	13.3924	80	0
45	1.3000	0.013892	11.827947	17.4535	90	5

TABLE B.2: Tabular Form of Data for t = 13 mm *(AYANLAR, 2004)*

Set	y_1 (cm)	Q (m^3/sec)	F_1	y_2 (cm)	L_J (cm)	x_J (cm)
11	1.0750	0.009643	10.918144	11.8364	75	25
12	1.1000	0.009643	10.548057	13.2387	60	5
13	1.1000	0.01128	12.338301	13.8620	70	85
14	1.1300	0.01128	11.850228	15.8615	65	35
15	1.7400	0.009612	5.284976	11.6806	43	5
16	1.5450	0.009612	6.3164661	10.5899	45	30
17	1.5800	0.011551	7.3395542	12.9271	70	40
18	1.4500	0.011551	8.3484012	14.6410	65	10
19	1.6600	0.009458	5.5808534	11.5248	45	20
20	1.8750	0.011802	5.8010385	12.3039	55	55
21	1.8050	0.011802	6.1417459	13.3945	60	30

TABLE B.3: Tabular Form of Data for Smooth Bed *(AYANLAR, 2004)*

Set	y_1 (cm)	Q (m^3/sec)	F_1	y_2 (cm)	L_J (cm)	x_J (cm)
24	2.2500	0.009346	3.4947767	14.9250	130	
25	2.1467	0.009346	3.7501298	16.5875	150	
26	1.9500	0.01099	5.0932151	16.1750	80	
27	2.0167	0.01099	4.8427579	17.3500	140	
28	2.5167	0.009316	2.9446921	15.0125	100	
29	2.4067	0.009316	3.1488684	16.7500	180	
30	2.2000	0.011302	4.3709312	16.3500	95	
31	2.7600	0.009561	2.6313239	12.4325	90	
32	2.6167	0.009561	2.8504625	12.9250	187	

33	2.8000	0.00954	2.5696129	11.6500	115	
34	1.8500	0.007366	3.6941633	9.7000	65	
35	1.9000	0.005544	2.6714711	6.1750	350	
36	1.4200	0.00951	7.0920324	17.6864	110	78
37	1.3000	0.010401	8.855496	16.0693	115	138
38	1.3000	0.010401	8.855496	17.2341	95	0
39	1.0000	0.009276	11.705467	18.1274	120	0
40	1.0500	0.009276	10.879397	15.6283	95	128
41	1.1650	0.010358	10.395442	18.5685	115	48
42	1.4000	0.01128	8.5931485	18.7155	95	0
43	1.3900	0.009622	7.4098565	15.8978	105	15

B-2. Experimental Data of EAD and RAJARATNAM (2002)

TABLE B.4: Tabular Form of Data for Ead and Rajaratnam (2002)

Experiment	t (cm)	y_1 (cm)	q (m^2/s)	F_1	y_2 (cm)	L_J (cm)
A1	1.3	2.54	0.051	4	10.4	41
A2	1.3	2.54	0.063	5	12.8	48
A3	1.3	2.54	0.076	6	14.5	54
A4	1.3	2.54	0.089	7	18.8	75
A5	1.3	2.54	0.101	8	20	85
A6	1.3	2.54	0.114	9	23.3	102
A7	1.3	2.54	0.127	10	26.3	109
B1	1.3	5.08	0.143	4	21	88
B1	1.3	5.08	0.207	5.8	31	129
C1	2.2	5.08	0.143	4	21	82
C2	2.2	5.08	0.207	5.8	31	129

B-3. Experimental Data of U.S.B.R. (1955)

TABLE B.5: Tabular Form of Data for Length of Jump (U.S.B.R. (1955)

F_1	L_J / y_2
1.8	3.9
2.1	4.4
2.22	4.6
2.4	4.8
2.8	5.2
3.2	5.5
3.58	5.7
4	5.8
5	6
6.5	6.13
7	6.16
7.5	6.17
8	6.18
9	6.15
10	6.1

APPENDIX C

CALIBRATION OF THE TRIANGULAR WEIR

The calibration of the triangular weir has been carried out by measuring the flow velocities in the upper flume. Assuming that the flow discharge is equal in each half of the flume, velocity measurements were done only for one half of the flume and the measured velocities were integrated numerically to obtain the discharge. For each discharge value, H, head on triangular weir was also measured. Calibration curve of the triangular weir was constructed with 8 different flow discharge and corresponding head values, H, measured far enough from triangular weir.

Velocity measurements of the stream were done with 4 pitot static tubes, attached on an apparatus, which can move along and across the channel. For an each discharge value, velocity measurements were done for 1 cm intervals from bottom to free surface and only the first measurement depth was 0.5 cm above the channel bed, because of the non uniform characteristic of the flow near the boundaries. So, depending on flow depth, different numbers of measurements were done in vertical direction.

At each depth, pitot static tubes were moved across the channel, from one sidewall of the channel to the imaginary center line of the channel and all measurement points in this direction are shown in Table. C.1.

In order to explain one set of the experimental procedure, measurement points in the flow cross sectional area for flow depth 6.48 cm (H=21.29) are given in Fig. C.1. For same flow depth, vertical velocity profiles of the flow 1.05 cm and 12.20 cm far from side wall off the channel are given in Fig. C.2. Horizontal velocity profiles of the flow 0.1 cm and 5.5 cm above the channel bed for flow depth 6.48 cm are given in Fig.C.3.

Table C.1: Points of Measurement across the Flume for each flow depth

Point	**1**	**2**	**3**	**4**	**5**	**6**	**7**	**8**	**9**	**10**	**11**	**12**
*	1.05	1.55	2.05	2.55	2.95	3.,05	3.45	3.55	3.95	4.05	4.45	4.55
Point	**13**	**14**	**15**	**16**	**17**	**18**	**19**	**20**	**21**	**22**	**23**	**24**
*	4.95	5.05	5.45	5.55	5.95	6.05	6.45	6.95	7.05	7.45	7.55	7.95
Point	**25**	**26**	**27**	**28**	**29**	**30**	**31**	**32**	**33**	**34**	**35**	**36**
*	8.05	8.55	9.05	9.55	10.05	10.55	11.05	11.20	11.55	11.70	12.05	12.20

**Distance from the Side Wall (cm)*

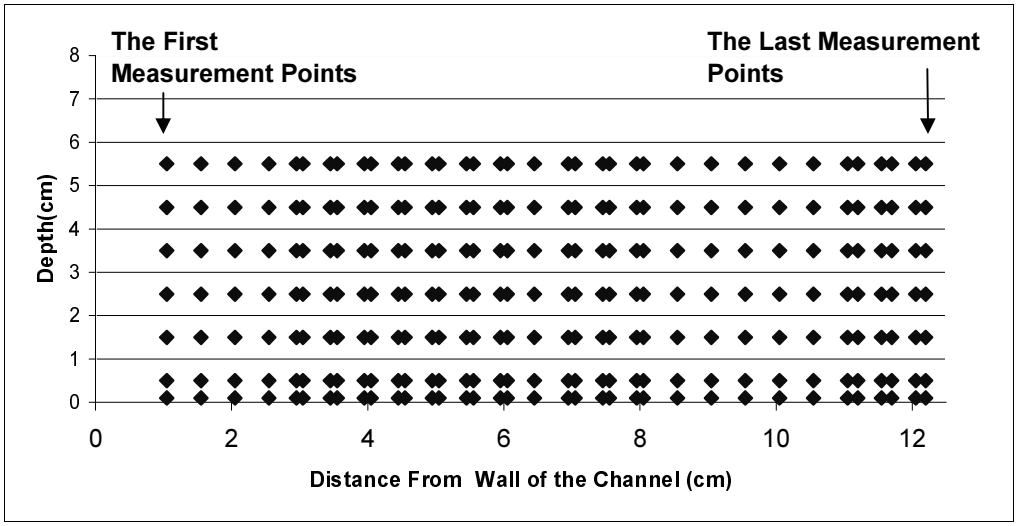

Figure C.1: Velocity Measurement Points on Cross Sectional Area

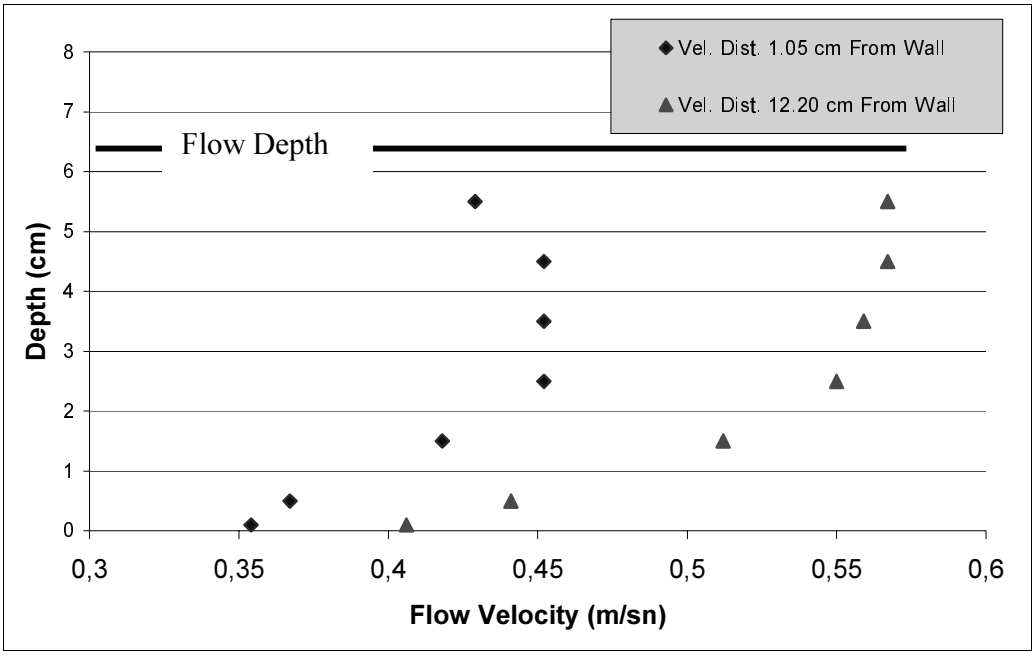

Figure C.2: Vertical velocity Distributions

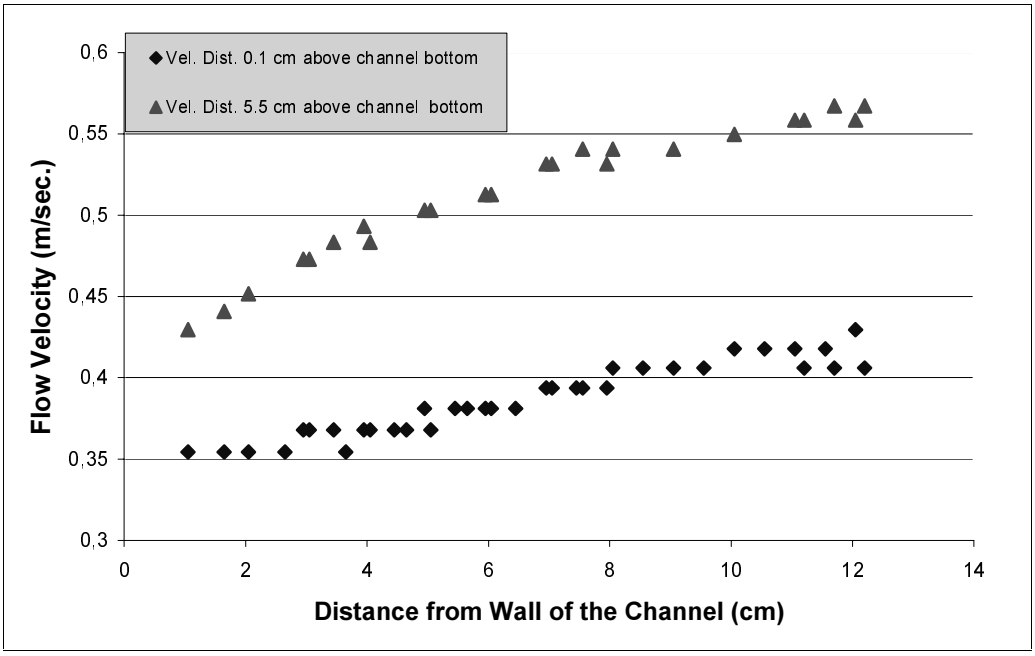

Figure C.3: Horizontal Velocity Distributions

To obtain discharge, effective areas of each measurement point were determined. Velocities at measurement points multiplied with effective areas of those points; hence flow discharge in the channel was calculated by summation of all calculated discharges on measurement points.

Results are shown in Table C-2 and they were compared with the discharge equation of the triangular weir, Eq. (3.1), to find the proper contraction coefficient C_C of the weir.

Table C.2: The Measured Head and Discharge on the Triangular Weir

H(cm)	Q(lt/sec.)
13.41	2.506
13.91	2.992
15.79	3.461
16.52	4.090
16.57	4.498
17.60	4.780
18.42	5.230
19.10	5.711
20.55	7.092
21.29	7.481

When measured discharge values were compared with those obtained from the theoretical equation of the triangular weir, the contraction coefficient, C_C was found to be close to 0.58. Hence, contraction coefficient was chosen as 0.58. The ratio values between measured discharges and theoretical discharges computed based on C_C=0.58 are given in Table C-3.

Table C.3: Ratios between Theoretical and Measured Discharges

H(cm)	Q theory / Q measured (Cc=0.58)
13.41	0.965
13.91	0.885
15.79	1.051
16.52	0.996
16.57	0.912
17.60	0.998
18.42	1.022
19.10	1.025
20.55	0.991
21.29	1.026